JOURNAL OF GEOPHYSICAL RESEARCH, VOL. 99, NO. B9, PAGES 17,805–17,825, SEPTEMBER 10, 1994

Effusive silicic volcanism in the Central Andes: The Chao dacite and other young lavas of the Altiplano-Puna Volcanic Complex

S. L. de Silva,[1] S. Self,[2] P. W. Francis,[3] R. E. Drake,[4] and Carlos Ramirez R.[5]

Abstract. The largest known Quaternary silicic lava body in the world is Cerro Chao in north Chile, a 14-km-long coulée with a volume of at least 26 km^3. It is the largest of a group of several closely similar dacitic lavas erupted during a recent (<100,000 year old) magmatic episode in the Altiplano-Puna Volcanic Complex (APVC; 21-24°S) of the Central Andean Volcanic Zone. The eruption of Chao proceeded in three phases. Phase 1 was explosive and produced ~1 km^3 of coarse, nonwelded dacitic pumice deposits and later block and ash flows that form an apron in front of the main lava body. Phase 2 was dominantly effusive and erupted ~22.5 km^3 of magma in the form of a composite couleé covering ~53 km^2 with a 400-m-high flow front and a small cone of poorly expanded pumice around the vent. The lava is homogeneous with rare flow banding and vesicular tops and selvages. Ogives (flow ridges) reaching heights of 30 m form prominent features on its surface. Phase 3 produced a 6-km-long, 3-km-wide flow that emanated from a collapsed dome. Ogives are subdued, and the lava is glassier than that produced in previous phases. All the Chao products are crystal-rich high-K dacites and rhyodacites with phenocrysts of plagioclase, quartz, hornblende, biotite, sphene, rare sanidine, and oxides. Phenocryst contents reach 40-60 vol % (vesicle free) in the main phase 2 lavas but are lower in the phase 1 (20-25%) and phase 3 (~40%) lavas. Ovoid andesitic inclusions with vesicular interiors and chilled margins up to 10 cm are found in the later stages of phase 2 and compose up to 5% of the phase 3 lava. There is little evidence for preeruptive zonation of the magma body in composition, temperature (~840°C), fO_2 (10^{-11}), or water content, so we propose that eruption of the Chao complex was driven by intrusion of fresh, hot andesitic magma into a crystallizing and largely homogeneous body of dacitic magma. Morphological measurments suggest that the Chao lavas had internal plastic viscosities of 10^{10} to 10^{12} Pa s, apparent viscosities of 10^9 Pa s, surface viscosities of 10^{15} to 10^{24} Pa s, and a yield strength of 8×10^5 Pa. These estimates indicate that Chao would have exhibited largely similar rheological properties to other silicic lava extrusions, notwithstanding its high phenocryst content. We suggest that Chao's anomalous size is a function of both the relatively steep local slope (20° to 3°) and the available volume of magma. The eruption duration for Chao's emplacement is thought to have been about 100 to 150 years, with maximum effusion rates of about 25 m^3 s^{-1} for short periods. Four other lavas in the vicinity with volumes of ~ 5 km^3 closely resemble Chao and are probably comagmatic. The suite as a whole shares a petrologic and chemical similarity with the voluminous regional Tertiary to Pleistocene ignimbrites of the APVC and may be derived from a zone of silicic magmatism that is thought to have been active since the late Tertiary. Chao and the other young lavas may represent either the waning of this system or a new episode fueled by intrusions of mafic magma.

Introduction

We describe here a group of large solitary, well-preserved silicic lava bodies from the Central Volcanic Zone of the Andes (CVZ; Figure 1). All are highly porphyritic, high-K dacites and rhyolites (Figure 2) and most have a steep-sided, circular plan and would be characterized as "low domes" [cf. *Blake*, 1990], while the others are coulées [cf. *Walker*, 1973]. These lava bodies are younger than most of the large late Pleistocene andesitic volcanoes that dominate the region. What makes these lavas exceptional is their large size. By far the most spectacular is Cerro Chao, a 14-km-long coulée with a flow front ~400 m high (Figure 3).

Located in northern Chile at 22°07'S, 68°09'W, Cerro Chao (also known as Volcan Chao or Chao lava) is a prominent feature of the Quaternary volcanic front, where its unusual squat character and morphology are in marked contrast to the older andesitic composite cones of Paniri and Leon which flank it (Figure 3). It was first described by *Guest and Sanchez* [1969], who estimated a minimum volume of 24 km^3. Such large volumes of silicic magma are usually erupted explosively to form ignimbrites, but large volume silicic lavas are known from several regions [e.g., *Henry et al.*, 1988; *Bonnischen and Kauffman*, 1987]. Unlike Chao, these are sheetlike, poorly exposed bodies, and in many cases their eruptive style is still debated [e.g., Henry and Wolff, 1992].

Apart from its sheer size, Chao poses several intriguing questions regarding its eruption, emplacement, and regional siginificance. Here we address these questions and present field observations that lend further insight into the eruption

[1]Department of Geography and Geology, Indiana State University, Terre Haute.

[2]Hawaii Center for Volcanology, Department of Geology and Geophysics, SOEST, University of Hawaii, Honolulu.

[3]Department of Earth Sciences, Open University, Milton Keynes, England.

[4]Berkeley Geochronology Center, Berkeley, California.

[5]Servicio Nacional de Geologia y Mineria, Santiago, Chile.

Paper number 94JB00652.
0148-0227/94/94JB-00652$05.00

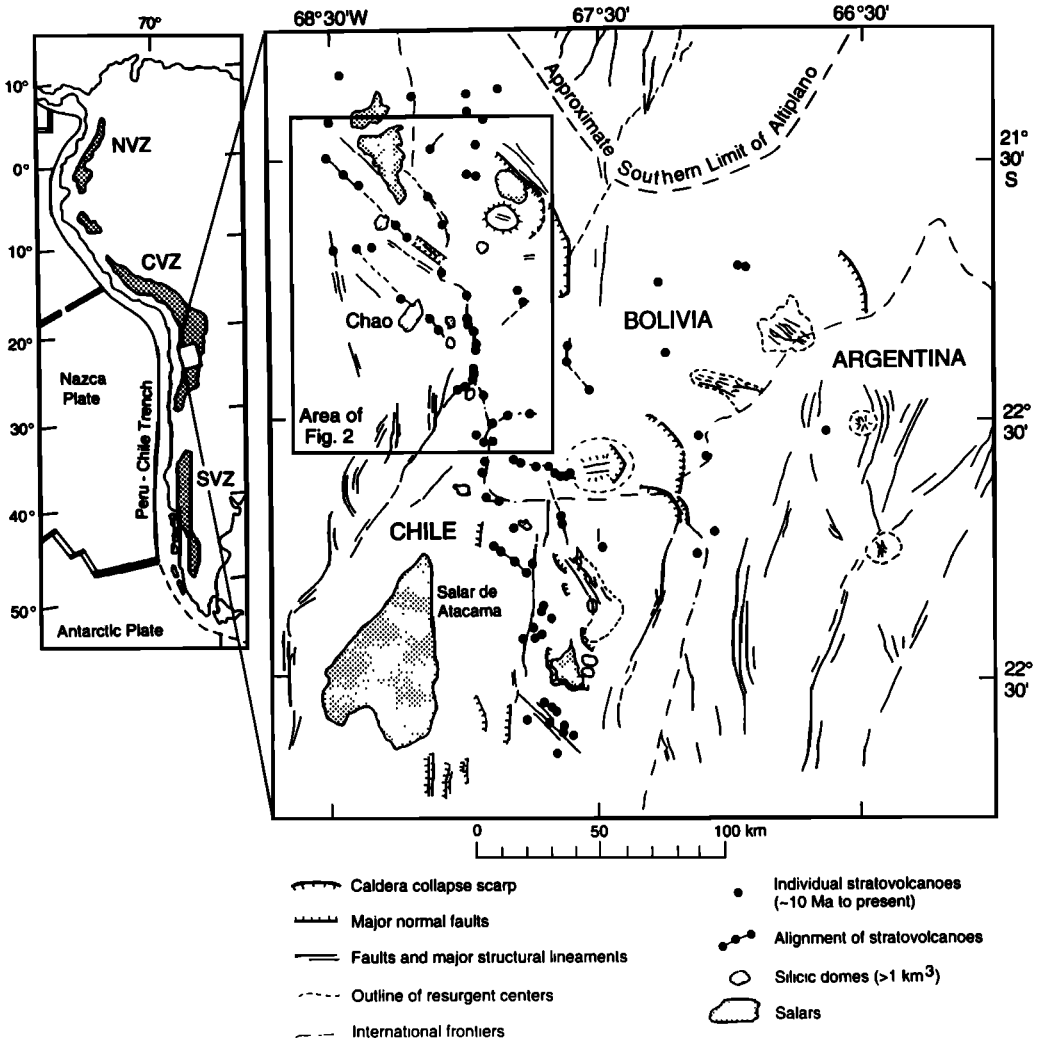

Figure 1. Altiplano-Puna Volcanic Complex of the Central Volcanic Zone (CVZ) of the Andes showing the major volcano-structural features. The region of young silicic lavas and domes described here is outlined and shown in Figure 2. Inset map shows distribution of the Cenozoic to Recent volcanic zones of the Andes and their relation to the plate tectonic framework of the western margin of South America. NVZ is Northern Volcanic Zone; SVZ is Southern Volcanic Zone.

mechanisms of the Chao crystal-rich dacite magmas, petrological data bearing on the origin of the magma, and the first geochronologic data. We estimate rheologic properties and effusion rate of the lava, and we present an integrated model for eruption and emplacement of the lava. We then compare Chao with other associated domes and volcanic rocks in the region and discuss their significance in the evolution of the Altiplano-Puna Volcanic Complex (APVC).

Geologic Setting

Chao and the associated domes are located within the APVC, a large zone of silicic volcanism occupying the 21° to 24°S segment of the Central Volcanic Zone of the Andes, which is one of three active volcanic zones in the Andes [*de Silva*, 1989a, and b; *de Silva and Francis*, 1991] (Figure 1). In the APVC, eruption of regionally extensive ignimbrites from several caldera complexes dominated the volcanic evolution from the late Miocene to the Pleistocene. Since then volcanism has been dominantly andesitic, forming large volcanic cones along a diffuse 50-km-wide volcanic front built upon the ignimbrite basement. Alignment of the volcanic front is approximately N-S, but the segment between about 22° and 23°S trends NW-SE. The location of the volcanic centers in this portion appears to be controlled by a series of NW-SE trending faults possibly related to the southern margin of the Pastos Grandes caldera complex (Figures 1 and 2). Chao is located on the easternmost arm of the NW trending portion of the volcanic front on a col between the volcanoes of Paniri and Leon (Figure 2).

Geochronology

Chao is clearly younger than the flanking volcanos of Paniri and Leon, on whose flanks it is constructed. A glacial moraine from Volcan Leon which abuts against the eastern flank of Chao forms part of a complex of moraines that terminate at about 4500 m. These moraines are thought to have been deposited during recession from the last glacial maximum [*Hollingworth and Guest*, 1967; *de Silva and Francis*, 1991]. On these grounds, Chao must therefore be older than ~11,000 years.

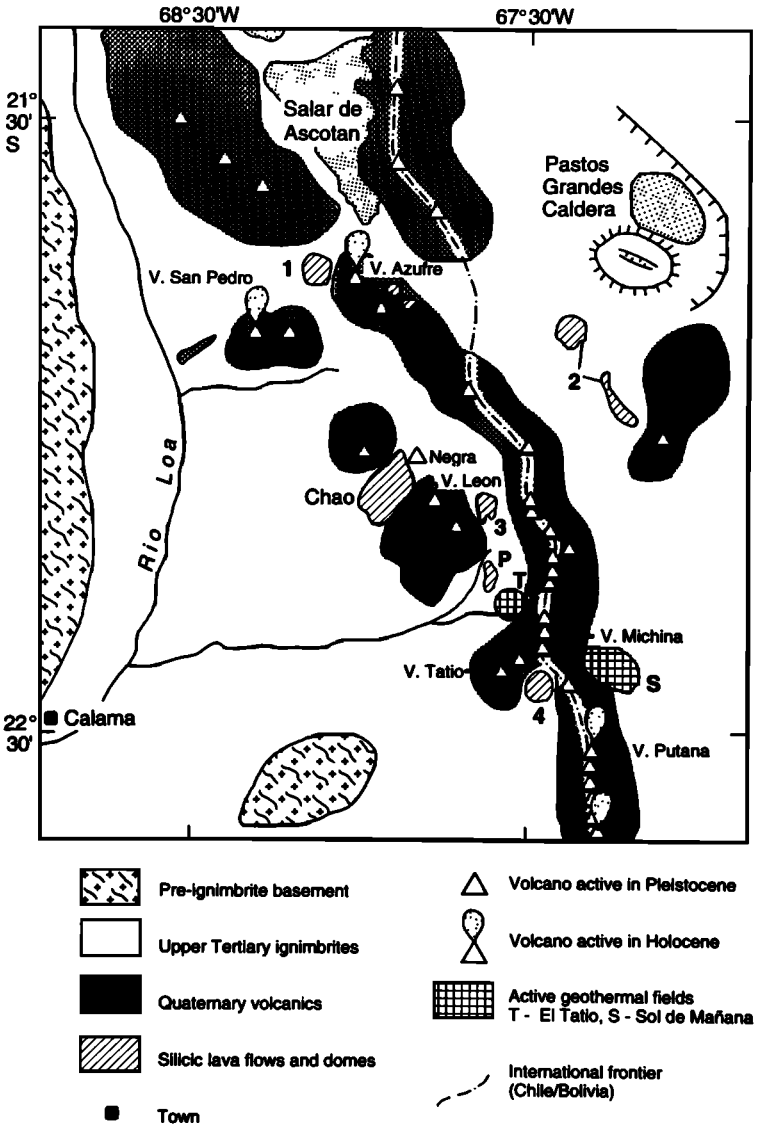

Figure 2. Map of the study area highlighting the volcanic geology. Locations of the Chao dacite and other young domes in relation to other major volcanic centers are shown. Centers numbered are 1, Cerro Chanka; 2, Chascon/Runtu Jarita; 3, Chillahuita; and 4, Tocopuri. P is Piedras Grandes a 7.5 Ma dome complex associated with the ignimbrites.

Three biotite separates from Chao I lava have been analyzed by conventional K-Ar and high precision $^{40}Ar/^{39}Ar$ single crystal laser fusion (SCLF) techniques (Table 1). An average age of 423,000 ± 100,000 years is suggested by the conventional method and may be a realistic age for Chao. However, individual crystals of biotite from each separate yielded anomalously old ages on SCLF dating. Thus, the K-Ar ages from the bulk separates could be considerably older than the true age. Anomalously old ages from single crystals may be the result of several causes, such as xenocrystic contamination, excess Ar, and K leaching. During microprobe investigations, several biotites with lower than normal totals and low K were found, suggesting that K leaching and alteration may have occurred in the Chao rocks. As a result, the age of Chao is not well constrained, but the SCLF data permit us to suggest that the age of Chao is less than the K-Ar age of 423,000 ± 100,000; how much less is unknown.

Geology

Pyroclastic Deposits

The most extensive erupted products from Chao are a previously unrecognized pyroclastic sequence that forms an apron 2-4 km wide and 3-4 km in extent beyond the southern flow front of Chao lava and is poorly exposed beneath the lava on the eastern side (Figures 3a and 3b). An unknown but potentially large volume of these deposits is thought to underlie the lava. We conservatively estimate the total dense rock equivalent (DRE) volume of these deposits to be approximately 1 km^3 .

Two groups of deposits are separated by an erosion surface and fluvial gravels (Figure 4). The older Chao pyroclastic flows are 10 to 15 m thick and nonwelded, and rest on fluvial sands and gravels and a 5-m-thick debris flow deposit composed of andesitic clasts, presumably derived from Paniri volcano. Large,

Figure 3a. Landsat Thematic Mapper (TM) image (Landsat 50522-14001 TM False Color Composite of bands 7,4, and 2 in Red, Green and Blue channels respectively) of 30 x 30 km portion of the Altiplano Puna Volcanic Complex showing Chao volcano and neighboring centers Paniri (P), Leon (L), and Sierra Negra (N). Note the ribbed surface of the 14-km-long Chao lava due to well developed ogives. Lava to the east is Cerro Chillahuita. These large silicic lavas contrast markedly with the ~6000-m-high, snow-capped, radially gullied and glaciated, central volcanoes of the Central Volcanic Zone. Note the approximate NW-SE trend of the front and the faults (F) that coincide with this.

poorly vesicular dacitic pumice blocks (maximum pumice (MP) ~1 m) and dense lava clasts similar in character and mineralogy to the juvenile material of the upper pyroclastic flows and Chao lava are abundant. The upper group of pyroclastic flow deposits are a series of coarse, fines-poor, nonwelded, pyroclastic flows (ignimbrite and block and ash flows) of limited extent with thicknesses of about 4-5 m where observed. Remnants of coarse pumice clast-rich flow ridges and flow fronts are present. Pumice clasts are dacitic, large (MP 2-3 m), and crystal rich. Coarse phenocrysts of quartz, plagioclase, biotite, and hornblende account for up to 30 vol % of the pumice and are set in a poorly to moderately vesiculated glassy matrix. Block (dense juvenile clasts with breadcrusted exterior) and ash flow units are more prominent in the upper part of the sequence. These dense clasts have identical petrology to the pumice blocks and the Chao lava itself.

Two overlapping pyroclastic cones located on the northern flank of Chao (Figure 3), constitute other evidence of explosive

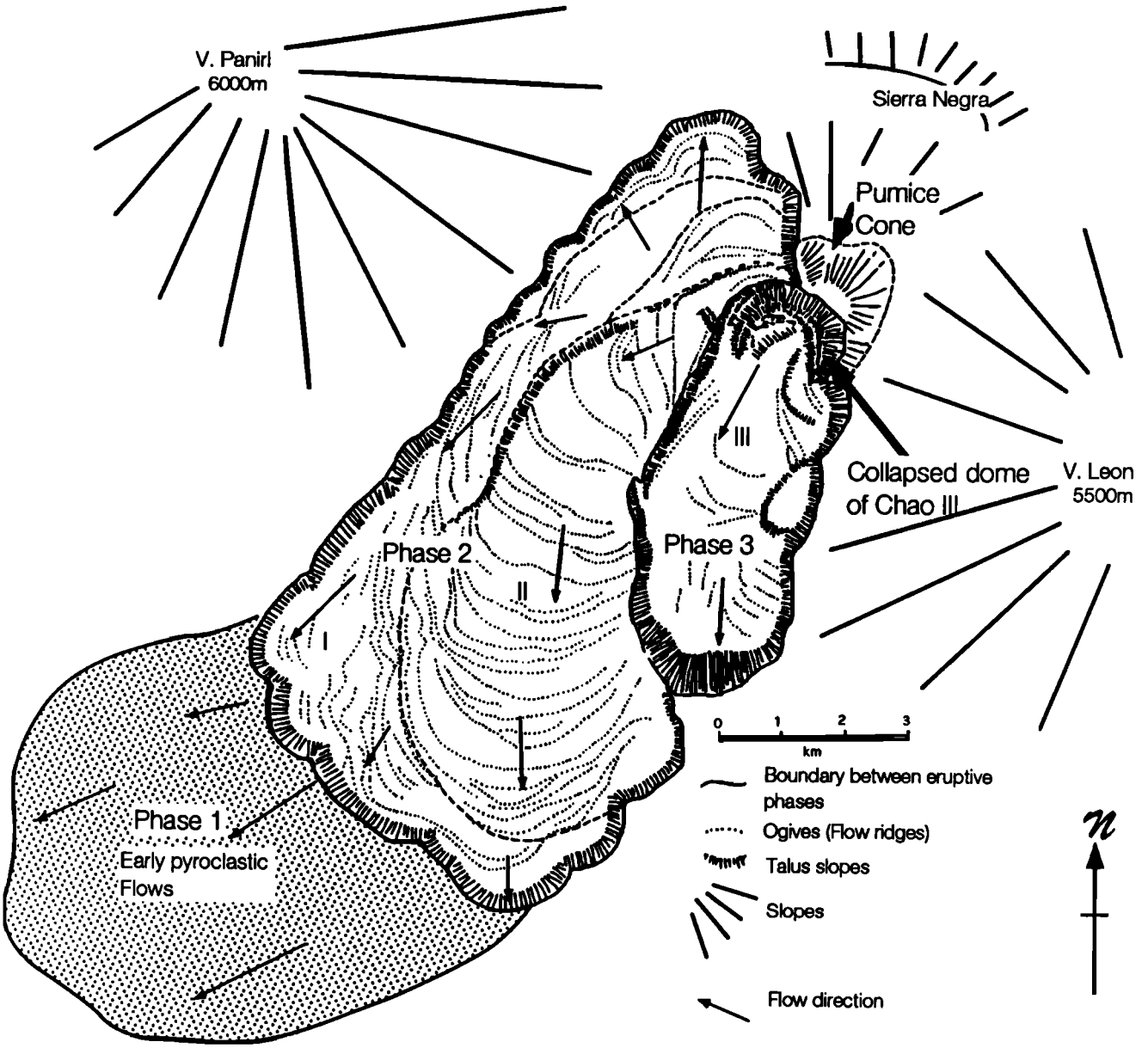

Figure 3b. Geologic sketch map of Cerro Chao, northern Chile. Main geologic features and neighbouring centers referred to in text are shown. Eruptive phases 1 through 3 are explained in text. Roman numerals I, II, and III refer to flow units of *Guest and Sanchez* [1969].

activity at Chao and mark the site of the vent for the eruption. A shallow depression filled with pumice blocks is found at the top of the cone. Its northern flank is steep and rises about 100 m from its base on the col between Leon and Paniri, and its location suggests a relatively high elevation for the vent; from here Chao lavas flowed into lower elevations to the west and south, filling in the topography. Although the middle Chao lava unit truncates the southern part of the pumice cone, pumice is found on top of the lava suggesting that the mildly explosive activity forming the pumice cone occurred throughout effusion of the main part of the Chao lava.

The cone is constructed of poorly vesicular pumice lapilli and blocks up to 30 cm. Plagioclase, quartz, biotite, and hornblende phenocrysts make up about 30 vol % of the rock. The matrix is a poorly expanded devitrified glass. The pumice is similar to the vesicular portions of the lava from Chao, although its density is somewhat higher (Table 2). Assuming a 3/4 cone with a diameter of 2 km, the DRE volume of the pumice cone is estimated to be 0.5 km^3.

In stratigraphic terms, eruption of the pyroclastic rocks marked the first, explosive phase of the eruption. Moderately explosive vulcanian to subplinian activity produced small, dense pyroclastic flows whose deposits accumulated to the south of the present lava. Erosional horizons within the sequence indicate that activity was semicontinuous. While most of the pyroclastic deposits are probably products of this early explosive phase, their similarity in composition and density to the Chao lava suggests that some of the uppermost block and ash flows may have been generated during part of the main extrusive event that produced the Chao lava, avalanching away from the front of the growing mass of lava. Thus the transition from phase 1 to 2 was gradual and was marked by a decline in pyroclastic flow emplacement. About 1 km^3 of magma was erupted during this phase.

A sparse layer of small pumice fallout lapilli is scattered over

Table 1a. Results of K-Ar Age Determinations of Biotite Separates from Chao I

Sample	K%	Radiogenic Ar^{40} nl g-1	Atmospheric Ar^{40} %	Age, Ma ± 2 σ
SO 985	6.82	0.08440	97.30	0.310 ± 0.263
SO 986	6.96	0.14430	95.60	0.533 ± 0.254
SO987	7.21	0.13160	93.00	0.470 ± 0.135

Samples were analyzed by S. de Silva at British Geological Survey Isotope Laboratory, London.

the surface of Chao, most prominently on the northern side. We originally thought this was associated with the pyroclastic cone on Chao [*de Silva et al.*, 1988]. However the pumice is mineralogically and chemically distinct from other Chao products and we now interpret this to be derived from the nearby Volcan San Pedro.

Chao Lava

We retain the subdivisions Chao I, II, and III established by *Guest and Sanchez* (1969) for the lower, middle and upper units of Chao lava (Figure 3b). Volume estimates given below are based on the profiles in Figure 5.

The lowermost coulée, Chao I, is the most extensive part of the Chao dacite. Major features of this 14-km-long lobe are its ~400-m-high flow front and the prominent flow ridges or ogives (see below and Figures 6a and 6b). The flow front is lobate, with lobe diameters ranging from 1.8 km on the distal margin to about 0.5 km on the northern side. Most of the flow moved southward, following preexisting topography, but lobate flow fronts on the northwest margin indicate that a component of the flow spilled over in that direction. Chao II directly overlies Chao I and is distinguished from it by a subdued scarp on its western side. The combined volume of Chao I and II is ~22 km^3, if a flat, uniformly sloping base is assumed. However, as indicated in Figure 4, the preexisting topography between Paniri and Leon volcanoes probably had a concave upward profile with a relatively steep headwall. In this region, the lower flanks of nonglaciated volcanoes typically have slopes of ~15-20°, grading downward into talus aprons with slopes of ~3 - 6° [*de Silva and Francis*, 1991]. Preeruption topography with these characteristics would therefore impart a considerably higher volume to the Chao complex.

Table 1b. Results of Ar^{40}/Ar^{39} single crystal laser fusion Technique for Biotite Separates from Chao I

Ar^{40}/Ar^{39}	Ar^{37}/Ar^{39}	Ar^{36}/Ar^{39}	Ar^{40*}/Ar^{39}	Percent Radiogenic	Age (Ma)	± 2 σ	Ar^{40}
			Sample SO 985				
22.86918	0.02656	0.07364	1.10861	4.8	0.387	± 0.120	7.265
18.68870	0.01692	0.06172	0.44848	2.4	0.157	± 0.108	4.863
18.18412	0.38870	0.05948	0.60772	3.3	0.212	± 0.080	6.393
22.06160	0.33690	0.07453	0.03901	0.2	0.014	± 0.087	3.660
19.76031	0.02711	0.07338	-1.92386	-9.7	-0.672	± 0.097	3.234
21.51208	0.10204	0.07666	-1.13400	-5.3	-0.396	± 0.116	2.237
			Sample SO 986				
221.42560	0.13654	0.74034	2.66501	1.2	0.931	± 1.131	15.692
23.87207	0.00746	0.07898	0.53098	2.2	0.186	± 0.225	2.414
33.19360	0.02524	0.11550	-0.93756	-2.8	-0.328	± 0.263	4.600
13.69843	0.01875	0.04771	-0.40211	-2.9	-0.141	± 0.100	1.306
26.86425	0.02481	0.09261	-0.50237	-1.9	-0.176	± 0.083	10.020
20.98473	0.02398	0.07252	-0.44563	-2.1	-0.560	± 0.064	14.086
			Sample SO 987				
6.86844	0.00427	0.02140	0.54232	7.9	0.189	± 0.105	1.342
32.54490	0.01652	0.06926	12.07863	37.1	4.216	± 0.312	1.728
17.03600	0.02781	0.06182	-1.23131	-7.2	-0.430	± 0.126	1.441
51.32864	0.00796	0.16614	2.23198	4.3	0.780	± 0.191	9.302
68.86053	0.03082	0.20169	9.26097	13.4	3.233	± 0.669	18.614

Samples were analyzed by R.E. Drake at the Berkeley Geochronology Center, Berkeley, California.

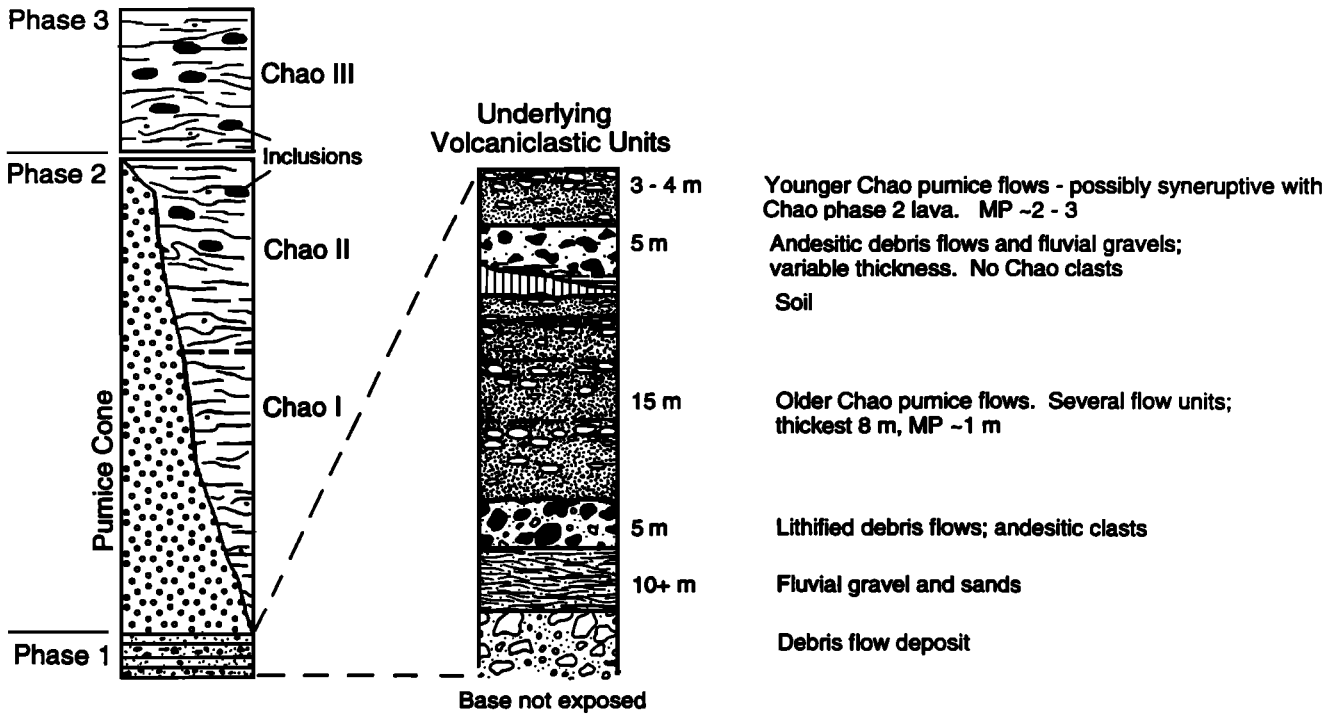

Figure 4 Composite eruption stratigraphy of the Chao dacite, built from traverses up the northern, eastern and southern flanks of Chao. MP is maximum pumice diameter. Columns are not to scale.

Macroscopically, Chao II and I are identical. Flow ridges up to 30 m high are prominent features on aerial and satellite images of Chao (Figure 3). Spacing between the ridges varies from 50 m near the flow front to as much as 100 m nearer the vent, where they are not so pronounced. Flow ridges on the western flank are stretched out parallel to the flow margin. The lava is massive, and remnants of vesicular flow tops and breccia zones are common but volumetrically insignificant. The upper vesicular surfaces of the lava are weathered and altered, causing it to disintegrate. On the northern flank of Chao II several 10 to 20-m mounds of lithified breccia are found on the tops of flow ridges close to the vent. These may represent fossil fumarole mounds.

Petrographically, both Chao I and II are monotonous crystal-rich dacites with prominent phenocrysts of quartz, plagioclase, biotite, and large hornblendes up to 2 cm. The porphyritic texture results from high but variable crystal contents (about 40 vol % on average but in some hand samples an almost holocrystalline texture is evident). Flow banding is ubiquitous. Toward the upper and northern (proximal) end of Chao II, small andesitic inclusions are common. These are typically small (up to 8 cm), ovoid or lobate, fine grained, and nonvesicular (Figure 6d). Some display glassy margins interpreted as chilled margins. These inclusions are not present in the areas of Chao I that were studied.

The distinction between Chao I and II made by *Guest and Sanchez* [1969] was largely morphological. There are several large ramparts on Chao I and II that could be interpreted as distinct flow lobes, but because of the similarity in lithology and petrology of the two lobes, rather than seeing these as representing hiatuses in activity, we suggest that they are merely manifestations of changes in the rate of lava extrusion and that Chao I and II represent pulses of the main eruptive phase of Chao (phase 2). At the vent, mildly explosive activity continued throughout effusion of the lava and built the pumice cone. About 22.5 km^3 of magma was erupted during this phase.

By contrast, the 6-km-long, 3-km-wide Chao III couleé appears distinct from Chao I and II, since it directly overlies the pumice cone in the north and Chao II on the eastern side. Its vent is marked by a collapsed dome that forms a steep-sided, crescent-shaped accumulation of blocky lava. Successive failures of this dome are indicated by several arcuate collapse scars on the inner wall of the crescent (Figure 3). The flow front of Chao III is a single convex lobe of blocky dacite, about 150 m high, with a smattering of the aeolian "sand" derived from weathering of Chao I and II. Ogives in Chao III are less obvious than on the lower lobes of Chao.

Chao III has a volume of about 3 km^3 and is typically dense blocky lava, with pumiceous zones common in its upper parts. Mineralogically, Chao III is similar to the rest of Chao but has a lower crystal content and a higher concentration of andesitic inclusions; up to 5 vol % of the rock in places. This is particularly evident about half way up the flow front. Many of the inclusions are larger (up to 20 cm) and more vesicular than those in Chao II, but are otherwise similar. Effusion of Chao III marked the third, final phase of the Chao eruption.

Table 2. Densities of Chao Lava and Pyroclastics

	Sample	Density kg/m^3
Pumice from upper pyroclastic flows	(#88069B)	845
Dense breadcrust clasts from upper pyroclastic flows	(#88069A)	2030
Pumice Cone	(#88080)	2340
Chao II vesicular lava	(#88069)	1710
Chao III lava	(#88067A)	2750
Chao II lava (slightly vesicular)	(#88081)	2030

Densities were determined by cutting cubes and weighing them (estimated accuracy is ± 30 kg/m^3).

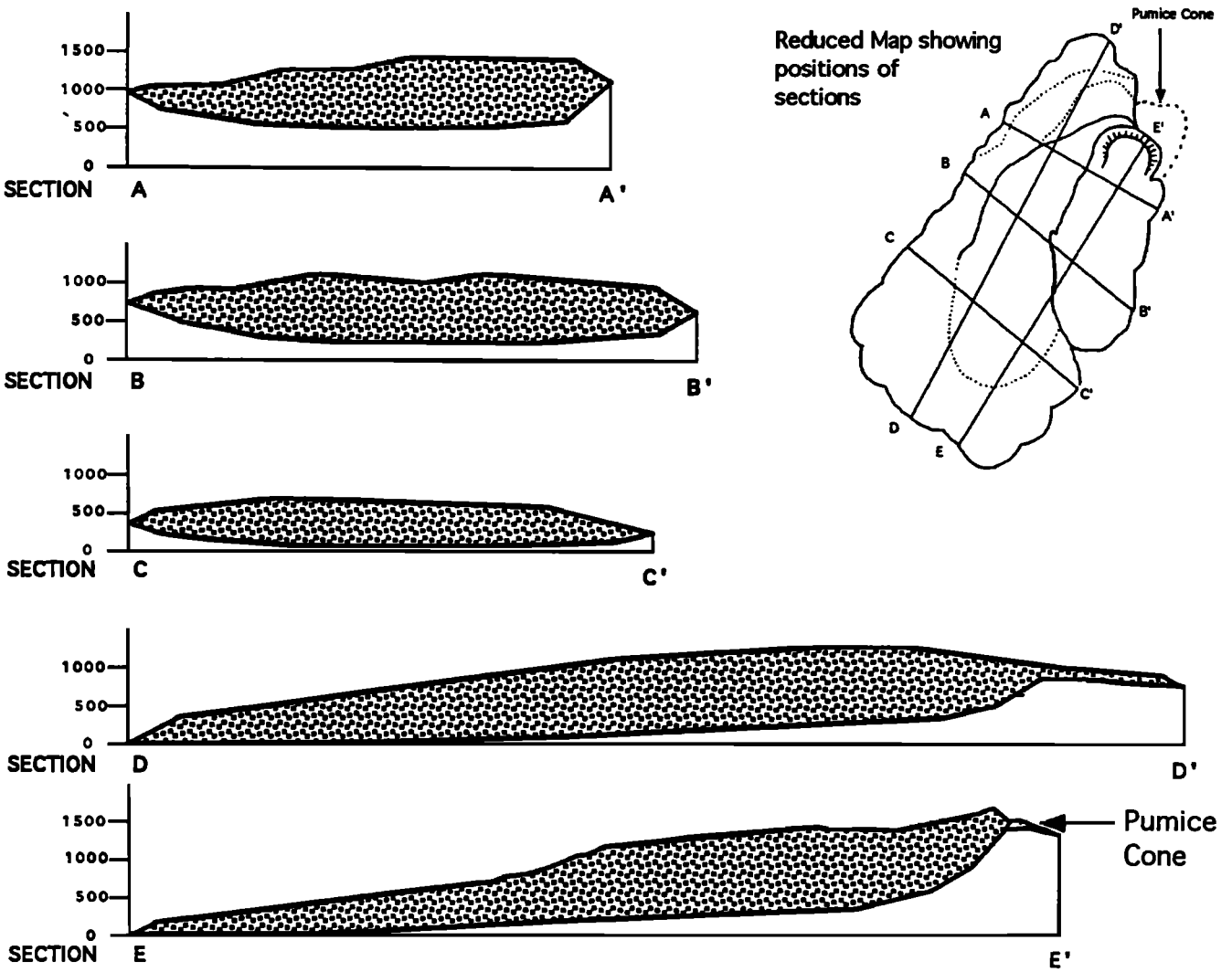

Figure 5. Profiles of the Chao dacite (modified from *Guest and Sanchez* [1969]). Heights are in meters above the basal flow front. Horizontal and vertical scales are equal.

Petrography, Mineral Chemistry, and Magmatic Conditions

Four representative samples from each major unit at Chao (pyroclastics, Chao I, II and III, and the inclusions) were chosen for detailed chemical and petrological studies. Sampling was conducted during traverses up the northern, southern, and eastern flanks of the volcano. The Chao rocks are all dacitic (dacites and rhyodacites), with phenocrysts of plagioclase > biotite > hornblende > quartz >> sphene > sanidine > Fe-Ti oxides. Apatite is the most common accessory mineral, both as microphenocrysts and as inclusions in the phenocrysts, together with zircon. Allanite was rarely detected. Phenocryst contents are variable, ranging from ~ 25 vol % (vesicle free) in the pumice to as high as 50 vol % in the lava. A phenocryst content of 40 to 45 vol % is typical for Chao (Table 3 and Figure 7a). Mineral chemistry was analyzed on a Cameca SX 50 electron microprobe at Purdue University. Data and operating parameters are available on request from the first author.

Plagioclase phenocrysts throughout Chao exhibit a variety of forms ranging from simple twins to complex reverse and normal zoning. Compositions throughout Chao are restricted with 90% of the range is between An_{26} and An_{55} (n = 100). Rarely, some cores as high as An_{63} are found. Quartz grains in Chao I and II are large with minor resorption; in Chao III quartz occurs as small embayed remnants of larger crystals. Phenocrysts of biotite are generally fresh in the massive lava but more altered in the vesicular samples. Large twinned hornblendes are common throughout Chao. Biotite and hornblende compositions show similar restricted ranges. Biotite phenocrysts and microlites throughout Chao are homogeneous with Mg number ranging from 58 to 60, while hornblendes are commonly zoned with cores and rims showing ranges of Mg numbers from 56-61 and 61-65 respectively. Hypersthene rimmed to varying extent by hornblende is found scattered throughout most thin sections of the Chao II lava. The hypersthene has Mg numbers of 80-83, identical to those in the andesitic inclusions (see below), and is thought to be xenocrystic. Glomerocrysts of hornblende and Fe-Ti oxides are probably resorbed pyroxenes.

In most of the dense lava samples, the matrix is a colorless high-silica rhyolite glass (Figure 7a) which in most of the lava samples is fresh. However, patches of spherulitic devitrification and variable K_2O and SiO_2 suggest alteration. Some samples also contain microlites of the phenocryst minerals that make up to about 50% of the matrix. The combination of the high phenocryst content and the partly crystallized groundmass leads to a very

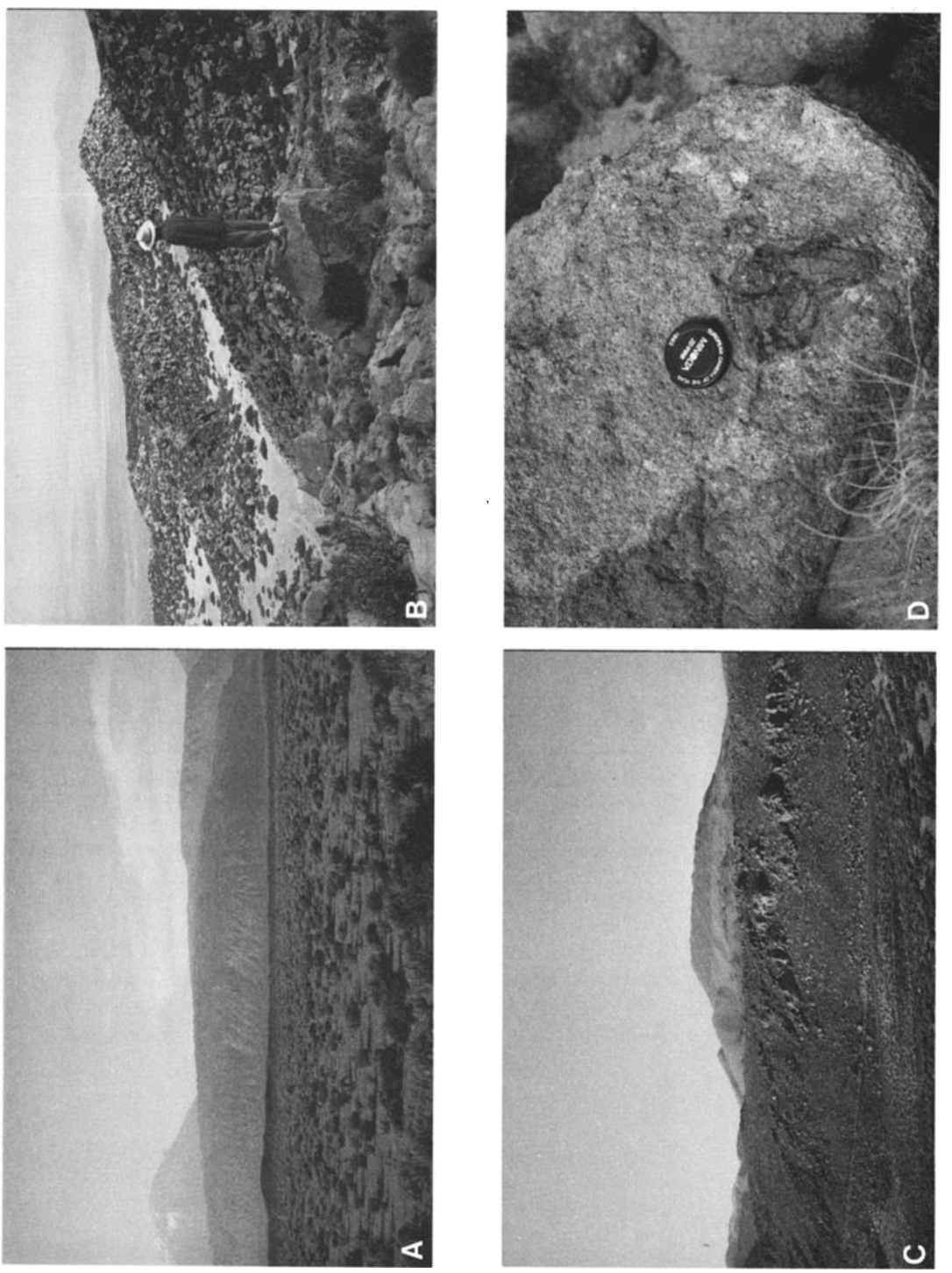

Figure 6. Field views of Chao volcano. (a) View north at the flow front of Chao. Snowcapped Volcan Paniri is to the west. Distance to the flow front is about 10 km. (b) Surface ridges or ogives of Chao II. Light material in the valleys is aeolian sand derived from weathering the lava. (c) Northern flank of Chao. Chao III forms skyline, overlying the lighter material of the pumice cone, with knobs of Chao II protruding through to the right of the cones. In the foreground is Chao I. (d) Andesitic inclusion in Chao II.

Table 3. Modal phenocryst data for samples from Chao

	Pyroclastics		Pumice Cone	Chao I		Chao II		Chao III	
	84063	88069C	88080	88073	84024	88068A	88068C	88081	88067
Rock Type	dense juvenile	pumice	pumice	lava	lava	lava	vesicular lava	lava	lava
Glass/Matrix*	60	65	60	55	50	47	57	57	55
Phenocrysts									
Plagioclase	18	17	17	19	21	22	21	18	21
Quartz	6	5	8	8	10	6	6	7	6
Biotite	7	7	5	9	7	9	7	8	7
Hornblende	4	2	8	5	7	10	6	7	7
Fe-Ti Oxide	1	2	1	1	2	1	1	1	2
Sanidine	2	1	1	2	nd	3	2	1	nd
Sphene	2	1	nd	2	2	2	tr	1	tr
Apatite †	tr	tr	tr	tr	tr	tr	tr	tr	1
Zircon †	tr	tr	tr	tr	tr	tr	tr	tr	tr
Allanite †	tr	tr	tr	nd	nd	tr	nd	nd	tr
Percent phenocrysts	40	35	40	45	50	53	43	43	45

All data are volume percent on the basis of 1000 points counted (analyzed by S. de Silva). Abundances for vesicular samples are calculated on a vesicle-free basis. Tr is trace and nd is not detected.

*Glass/matrix is treated as noncrystalline material in this data set

† These minerals were detected only as discrete microphenocrysts or as inclusions

high overall crystal content for Chao (>60%). In a few samples the groundmass is devitrified to a fine-grained aggregate. In the vesicular samples, the glass is largely devitrified and dusty, although rare fresh patches are found.

Andesite inclusions in Chao II and III are sparsely porphyritic with a few large crystals of plagioclase, hypersthene, quartz, biotite, and hornblende set in a groundmass of randomly oriented acicular hornblende, plagioclase, and euhedral hypersthene surrounded by a small proportion of glassy mesostasis. Of these groundmass minerals, plagioclase shows a range of An_{65} to An_{74}, hornblendes have Mg numbers ranging from 65-68, and hypersthenes have Mg numbers of 80-82. The glassy mesostasis is high silica rhyolite. Of the large crystals in the inclusions only hypersthene appears to be in equilibrium. Quartz is highly resorbed and has reaction rims of augite (Figure 7c), plagioclase is commonly highly fretted and shows reaction on its rims, and both biotite and hornblende phenocrysts exhibit breakdown to an aggregate of oxides and smaller crystals. A large (1 cm) hornblende lath (Figure 7d) in the inclusion has a core composition typical of the Chao dacite (Mg number of 60.5) and a rim typical of the andesite (Mg number of 67.4). It is likely that these large crystals are actually xenocrysts inherited from the Chao dacite magma, as at Cerro Purico [*Davidson et al.*, 1990] and Chaos Crags [*Heiken and Eichelberger*, 1980].

Compositions of coexisting Fe-Ti oxides indicate little variation in temperatures (~840 °C) and fO_2 (10^{-11}) throughout the magma (Table 4). Total pressure estimated using the method of *Johnson and Rutherford* [1989] indicates a P_{tot} of ~0.2 GPa (2 kbars) indicating that the magma equilibrated at about 7 - 8 km. *Naney* (1983) suggests that at these pressures, the presence of both hornblende and biotite indicates H_2O contents of at least 4 - 5 wt% in magma. For a crystal-rich magma such as Chao, preeruption H_2O contents in the magma (liquid plus crystals) would have been ~2 wt %.

Whole Rock Composition

Whole rock analyses of the the Chao products show that the magma was calc-alkaline, high-K dacite (Table 5). There is little variation from phase 1 through 3 for major or trace elements, indicating a homogeneous magma batch (Figure 8). SiO_2 varies from 66.97 to 69.77 wt %, K_2O from 3.73 to 3.94 wt %, Rb from 162 to 170 ppm, Sr from 282 to 327 ppm, and Th from 28 to 29 ppm. The andesite inclusions are more mafic with lower Rb, Th, and Nb and significantly higher Cr, Sr, Y, and Zr; Ba is marginally higher. A single representative sample of Chao I lava (sample 84054) was found to be LREE enriched, with a Ce/Yb of 48, an $^{87}Sr/^{86}Sr$ ratio of 0.70805, and a $^{143}Nd/^{144}Nd$ ratio of 0.512247.

The scattered pumice lapilli airfall found on the surface of the Chao lava is anomalous in petrologic and chemical character. It is sparsely porphyritic with plagioclase, augite, and hypersthene phenocrysts set in a clear vesicular glass matrix. Plagioclases are more calcic (An_{75} to An_{80}) and the glass more mafic (~70% SiO_2) than any of the volcanic products demonstrably of the Chao volcano. It is more mafic than the dacites of Chao, and although its major element composition may be generated by mixing between the andesitic inclusions and dacitic lava of Chao, its trace element characteristics are inconsistent with such an origin. High Ba and Sr and low Th contents, in particular, are more typical of the pumice falls erupted from the nearby San Pedro volcano [*O'Callaghan and Francis*, 1986], which was the most probable source.

Physical and Rheological Parameters

Our observations indicate levels of crystallinity (40 to 60%) close to the critical limit for silicic magmas [cf. *Marsh*, 1981]. This raises interesting questions about the influence of high crystal content on the rheological and physical properties of silicic lavas. We have estimated various physical and rheological parameters for Chao (Table 6). Chao has an aspect ratio of ~20, which falls at the extreme end of the known range for other silicic lavas [*Henry et al.*, 1988], a yield strength of 8×10^5 Pa s, internal plastic viscosity in the range 10^{10}-10^{12} Pa s, and surface viscosity in the range 10^{15}-10^{24} Pa s. These are not exceptional for silicic lavas. Further, using the method of *Pinkerton and Stevenson* [1992], we obtain an estimate of 10^9 Pa s for the

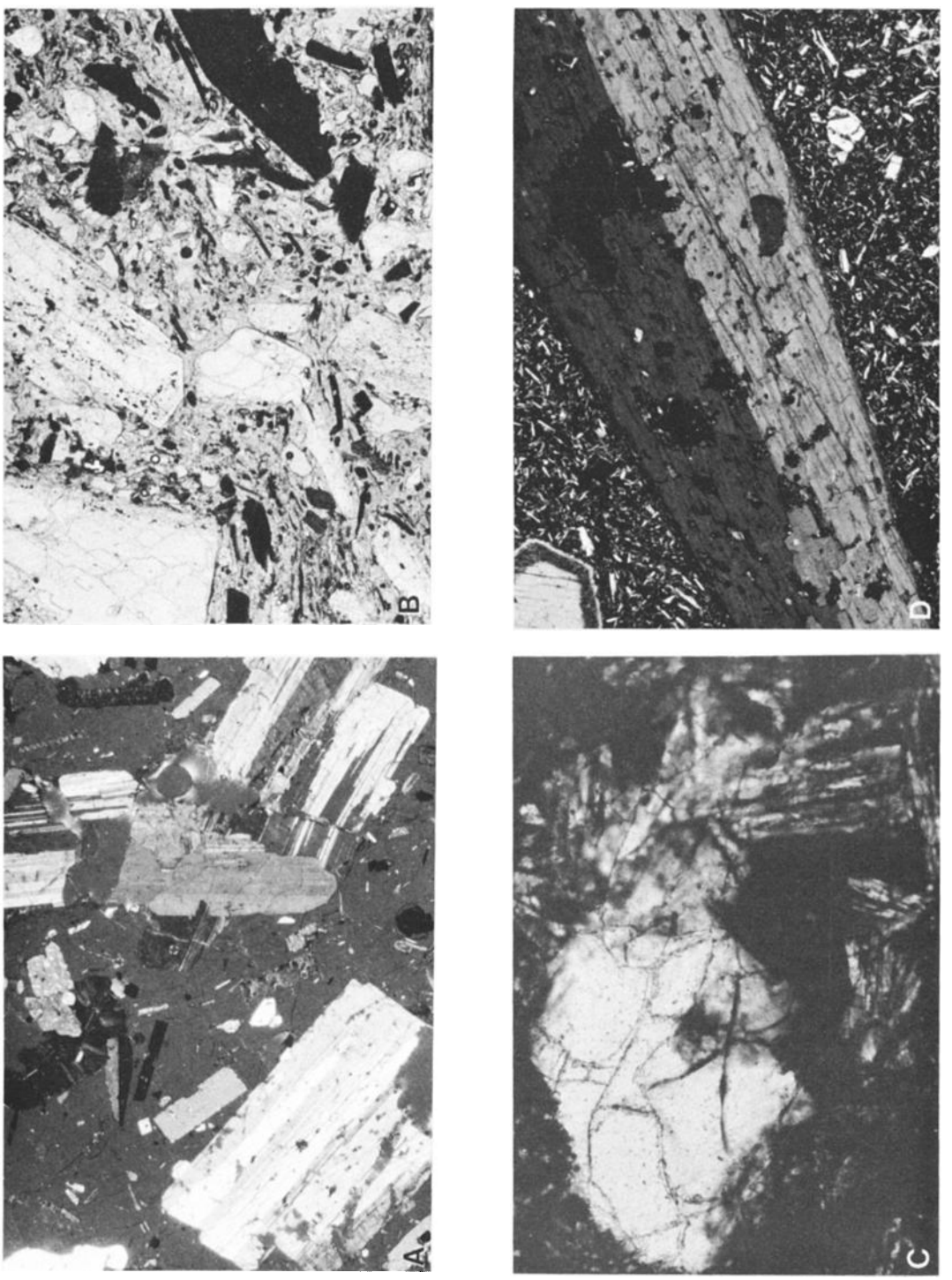

Figure 7. Photomicrographs of Chao (XPL is crossed polars, PPL is plain polars, FOV is field of view): (a) Chao I lava, partial XPL, FOV 4 mm. Phenocrysts are plagioclase, biotite, and hornblende in fresh glass matrix. Note areas of incipient devitrification in upper left quadrant. This sample has a crystal content of ~54%. (b) Vesicular Chao II lava, PPL, FOV 4mm, with phenocrysts of quartz, plagioclase, biotite, and hornblende, set in a partly devitrified vesicular glassy matrix. (c) Large quartz xenocryst with acicular clinpyroxene XPL, FOV 0.5 mm. Sample is an inclusion from Chao III. (d) Large hornblende xenocryst in andesitic inclusion, set in seriate textured fine-grained matrix with glass (XPL, FOV 6 mm).

Table 4. Temperature and fO_2 Estimates Based on Fe-Ti Oxide Compositions

	Phase 1		Phase 2		Phase 3	
	Mag	Ilm	Mag	Ilm	Mag	Ilm
SiO_2	0.06	0.02	0.00	0.00	0.00	0.00
TiO_2	4.30	34.19	4.88	35.72	4.56	34.67
Al_2O_3	1.11	0.23	1.56	0.41	1.40	0.14
FeO	84.47	60.81	85.35	58.01	85.89	57.52
MnO	0.54	0.41	0.56	0.85	0.52	0.71
MgO	0.60	0.58	0.69	1.29	0.86	1.34
CaO	0.10	0.15	0.07	0.05	0.04	0.04
NaO	0.12					
Subtotal	91.30	96.39	93.11	96.33	93.27	94.42
FeO*	32.78	29.32	33.84	28.96	33.38	28.07
Fe_2O_3*	57.44	35.00	57.25	32.28	58.35	32.73
Total	97.06	99.90	98.85	99.56	99.12	97.70
log (Mg/Mn)	0.29	0.40	0.34	0.43	0.46	0.52
X(usp)†	0.13		0.15		0.14	
X(ilm)†		0.66		0.68		0.67
T°C ‡	853.80		864.92		855.23	
log fO_2	-10.33		-10.30		-10.37	
T°C ¶	826.20		832.11		827.15	
log fO_2	-11.22		-11.24		-11.25	

Mag is magnetite (spinel), and Ilm is ilmenite (rhombohedral). Oxides are in weight percent. Usp is ulvospinel.

*Calculated assuming charge-balanced stoichiometric formula.

†Calculated following *Stormer* [1983].

‡ Calculated following *Spencer and Lindsley* [1981].

¶ Calculated following *Anderson and Lindsley* [1985].

apparent (bulk) viscosity, similar to that calculated for the Mount St. Helens dome, another crystal-rich silicic lava body. The yield strength calculated in Table 6 is approximately an order of magnitude higher than expected for magmas of this composition at magmatic temperatures [cf. *McBirney and Murase*, 1984] but is similar to values calculated for other domes and couleés. Formation of a viscous carapace, as indicated by the well-developed ogives, was probably an important factor in this elevated yield strength estimate [e.g., *Blake*, 1990]. *Griffiths and Fink* [1993] propose that the strength of the crust, where well developed, is more significant than the physical properties of the internal part of the lava body in controlling morphology and distance flowed.

Chao was erupted onto an average slope of about 4°, although the slope may locally have been as great as 20°(see below). This slope strongly influenced the growth and final morphology of the Chao lava. For magma with a yield strength erupted onto a slight slope, *Blake* [1990] suggests that for coulées to form, the condition

$$R > h_0/\sin^2 \theta$$

must be satisfied, where R is the dome radius, h_o is the natural length scale, and θ is the slope. At Chao where R =4 and $h_0/\sin^2 \theta = 1.26$, the condition above was satisfied and coulée formation resulted. *Blake* [1990] also predicts that the material first piles up near the vent to form a symmetrical lava dome; when the dome collapses, a short coulée forms. This appears to be the sequence of events shown by Chao III, which was emplaced onto the upper surface of Chao II on a slope of about 2°. The diameter of the dome appears to have been about 1.5 km before it yielded to form a coulée, indicating a yield strength of 5×10^5 Pa according to the method of *Blake* [1990, Figure 14]; this value is consistent with our morphological estimate.

During the first phase of the Chao eruption, lava probably erupted onto a much steeper slope, possibly as much as 15 to 20°. On these slopes, any initial dome would have achieved only very small size (100-200 m in radius) before collapsing and would not readily be detectable. Some of the upper pyroclastic flows probably formed as a result of collapse from such a nascent dome.

Our estimates show that although Chao magma was extremely crystal rich, its rheological properties are typical of silicic lavas in general. This runs counter to the conventional view that increased crystallinity results in increased bulk viscosity, leading to the system locking up when a critical crystallinity of ~40 to 60% is reached [cf. *Marsh*, 1981]. The fact that many lavas with crystal contents close to or greater than the critical limit exist implies that factors other than the crystal content are important. It is possible that while higher crystal content leads to increased bulk viscosity,

Table 5. Representative Analyses of Major and Trace Elements of Chao Lava and Pyroclastics

	Phase 1		Phase 2						Phase 3			San Pedro
	84063	88069C	88080	88073	84024	88068A	88068C	88069	88067	88081	88068B	88085
Type/ Source	Dense Juvenile	Pumice from flow	Pumice Cone	Chao I	Chao I	Chao II	Vesicular Chao II	Chao II	Chao III (South)	Chao III (North)	andesite	Plinian airfall
SiO_2	68.61	69.06	66.97	69.77	69.20	67.71	69.08	68.07	68.10	67.80	60.31	64.34
TiO_2	0.52	0.48	0.54	0.52	0.51	0.52	0.46	0.49	0.50	0.54	0.87	0.70
Al_2O_3	14.95	14.82	16.05	14.12	14.65	15.48	15.27	15.57	15.33	15.29	17.30	16.85
Fe_2O_3	3.65	3.39	3.77	3.63	3.56	3.63	3.06	3.44	3.54	3.80	6.14	4.68
MnO	0.07	0.06	0.06	0.06	0.07	0.06	0.06	0.06	0.06	0.06	0.09	0.07
MgO	1.62	1.51	1.79	1.68	1.60	1.72	1.39	1.58	1.68	1.83	3.76	2.09
CaO	3.61	3.49	3.73	3.23	3.45	3.70	3.40	3.67	3.61	3.61	5.83	4.27
Na_2O	3.15	3.09	3.18	3.09	2.96	3.24	3.19	3.23	3.28	3.08	3.09	3.82
K_2O	3.68	3.96	3.73	3.78	3.87	3.75	3.94	3.76	3.75	3.78	2.39	2.92
P_2O_5	0.14	0.13	0.21	0.12	0.13	0.13	0.15	0.12	0.14	0.21	0.23	0.24
LOI	1.67	2.46	1.90	2.69	2.30	1.40	2.28	2.38	1.07	1.40	1.84	3.80
Rb	169	166	162	162	163	166	170	162	168	168	78	90
Sr	325	321	326	282	314	318	323	327	317	319	493	502
Ba	613	654	626	593	635	615	638	605	606	640	678	838
Y	16	15	16	15	15	17	13	16	16	16	20	15
Zr	146	141	146	146	148	141	139	147	143	148	185	193
Nb	12	12	12	12	12	12	11	13	12	12	11	10
Th	28	28	28	29	29	28	28	29	29	29	12	10
Ni	13	10	14	11	12	11	11	11	12	13	18	20
Cr	41	34	42	41	38	42	32	43	42	47	100	39

Major elements were recalculated to 100 wt %. LOI is loss on ignition. Other elements are given in parts per million. Samples were analyzed at University of Hawaii, at Manoa (analyst: T. Hulseboch) except for samples 84063 and 84024 which were analyzed at University of Southampton, England (analyst: I. W. Croudace).

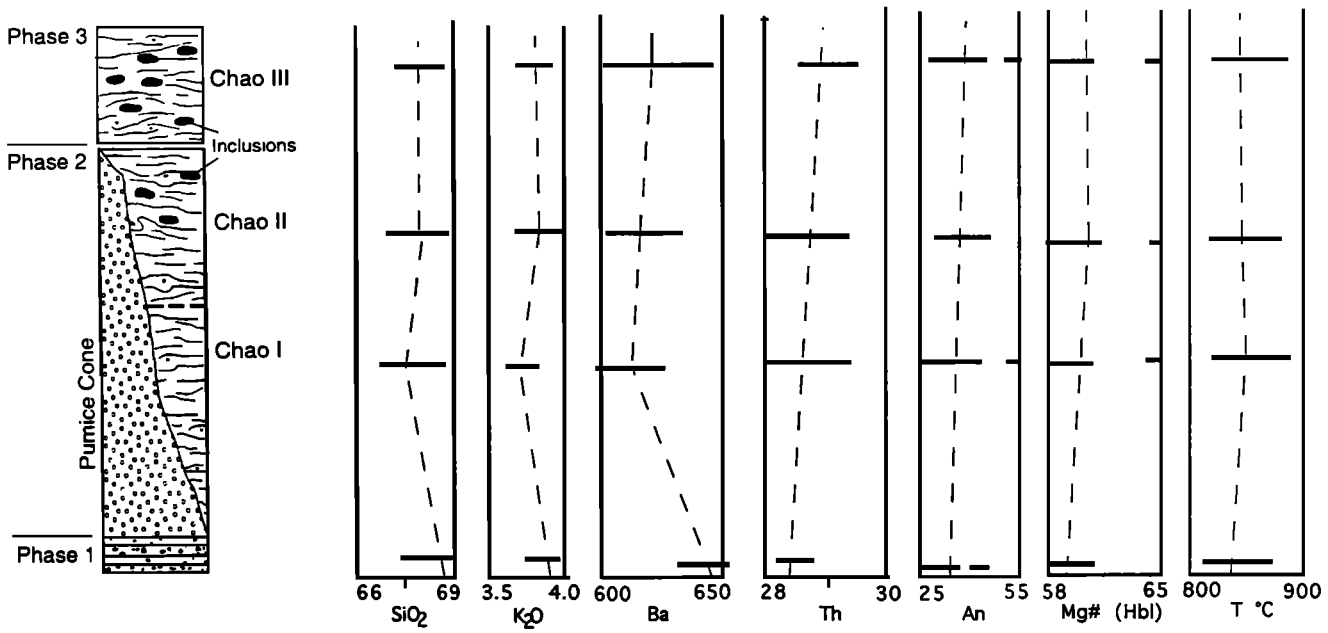

Figure 8. Variation of petrological and chemical indicators with eruption stratigraphy (see Figure 4). Only the juvenile compositions are plotted. Data shown are from 16 samples of Chao (inclusions not included), four samples from each unit. Horizontal bars indicate range of analyses for each unit, and dashed vertical lines join mean values.

the resulting increase in yield strength coupled with the growth of a crust reduces heat loss, which in turn reduces the bulk viscosity [e.g. Dragoni and Tallarico, 1994]. The massive ogives on the surface of the Chao lavas indicate that the carapace was thick and strong, so it is possible that the yield strength-temperature relationships may have outweighed the effect of crystal content in determining the overall rheology of the Chao lavas.

Eruption Duration and Growth Rate of Chao

Although Chao was erupted in three stages, each stage appears to have been continuous. For instance, the Chao I / II coulée shows little evidence of breaks in activity, although there may have been variations in the effusion rate as suggested by ramparts. Intuitively, a steady supply of magma would have been needed to keep the flow moving. This leads us to questions about the rate of magma supply, eruption duration, and growth rate. Unfortunately, such questions are not easily answered for prehistoric flows because of the errors in translating morphologic characteristics into kinetic process variables and because of the subtle but important difference between effusion rate (flux at the vent regardless of density, V_f) of magma at the vent and eruption rate (DRE or mass equivalent per second, V_e) estimated from degassed and solidified lava. Nevertheless, we attempt to provide some insight into these questions below.

We use morphometric parameters to estimate growth rates because these are the least problematic for our purposes. *Kilburn and Lopes* [1991] used data from historic eruptions to proposed the following empirical relationship between growth rate and morphometric parameters of lava fields:

$$(W_m/L_m)H^2 \sin \alpha = 0.1T \qquad (1)$$

where W_m is the maximum width, L_m is the maximum length, H is the mean depth of the flow, α is the slope, and T is the time (days). This approach is one of the few apparently composition-independent relationships in the literature (most of the others deal with exclusively mafic flows) and it allows an estimation of the time required for a lava field to achieve specified dimensions. For Chao I and II, the measured morphological parameters are $W_m = 7 \times 10^3$ m; $L_m = 14 \times 10^3$ m; $H = 500$ m, and average α of 4° (see above); these parameters yield T, the eruption duration, as about 250 years. This implies growth rates of 2 to 3 $m^3 s^{-1}$ for the main phase of Chao.

Our calculated growth rate is typical of historically observed domes worldwide like Mount St. Helens [*Swanson et al.* 1987] and Santiaguito [*Rose*, 1987]. Further, *Manley* [1992] suggests that durations of hundreds of years are not unreasonable for cooling (and perhaps flow) of sheetlike silicic lava bodies. Nevertheless, we consider the estimate of the eruption duration to be an overestimate for Chao. First, there is considerable scatter in the Kilburn and Lopes data, and the errors associated with the analysis are ~ 70% for the left hand side and 10% for the right hand side of equation (1). The errors are of the order of the uncertainties in measurements of some of the parameters at Chao, particularly depth and slope. Further errors are introduced for large-volume eruptions like Chao because their relationship needs to be extrapolated beyond the bounds of the data. Second,

Table 6. Estimates of Rheological Properties of Chao Lava

	Value	Method
Internal plastic viscosity	10^{10} - 10^{12} Pa s	*Moore et al.* [1978]
Surface viscosity during folding	10^{15} - 10^{24} Pa s	*Fink* [1980]
Yield Strength	8×10^5 Pa s	*Blake* [1990]
Aspect ratio (H/V)	20	*Walker* [1973]

H is the diameter of circle with the basal area of the lava, and V is the thickness of the lava.

although the growth rates are appropriate by analogy with the historic domes, these grow exogenously in a series of eruptive episodes followed by periods of stasis, whereas the main phase of Chao (24 km^3) appears to have grown endogenously during a single eruptive episode. During an eruptive episode the effusion rate peaks soon after the beginning of the eruption and then gradually drops to lower values as the eruption proceeds [e.g., *Wadge*, 1981; *Stasiuk et al.*, 1993]. The main volume of a lava may therefore have been effused in a very short period of time, but the last few percent may have taken a considerably longer time.

To obtain a more realistic estimate of the eruption duration at Chao an estimate of the effusion rate is required. This may be done by using one of the available fluid dynamic and thermal models [e.g., *Huppert et al.*, 1982; *Fink and Griffiths*, 1992; *Stasiuk et al.*, 1993]. However, these are more appropriate for interpreting flows and domes with detailed records of effusion and morphologic evolution, and they involve several variables that are poorly constrained in prehistoric flows like Chao. A less problematic approach is to use the dimensionless Graetz number that is related to the cooling of a warm fluid moving through a cold pipe. This is commonly used to calculate effusion rates for flows where only morphometric parameters are available [e.g., *Hulme and Fielder*, 1977; *Wilson and Head*, 1983] and therefore may be appropriate for our purposes. Essentially,

$$V_f = 300\,\kappa W L / H$$

where, W, L, and H are as in equation (1), and κ is the thermal diffusivity ~ 5 x 10^{-7} m^2/sec ($\kappa = K / \rho_D c_p$; values for K (thermal conductivity), ρ_D (nonvesicular lava density), and c_p (specific heat capacity) are 1.26 J m^{-1} s^{-1} K^{-1}, 2750 kg m^{-3}, and 1150 J kg^{-1} K^{-1} respectively). This yields effective eruption rates of about 25 m^3 s^{-1}. This translates to an eruption duration of about 20 years for Chao. We believe this duration to be an underestimate, because the Graetz number approach assumes a continuous steady state eruption and thus ignores variables such as changes in conduit diameter and local slope and any changes in effusion rate that may have occurred during the eruption. We suggest that the Graetz number approach yields eruption rates close to the peak value for Chao. This is not unreasonable when compared to Mount St. Helens, where in individual eruptive episodes from June 1980 to August 1982, eruption rates ranged from 2 to 26 m^3 s^{-1} [*Swanson et al.*, 1987, Table 1].

Our analysis illustrates the difficulties in estimating eruption parameters for pre-historic flows like Chao. We have used what we consider to be the most appropriate models and obtained results which are an order of magnitude different. The difference is rooted in the different approaches of the two models; the *Kilburn and Lopes* [1991] approach yields an eruption duration that includes periods of stasis and is therefore an overestimate, while the Graetz number approach assumes a continuous eruption and therefore underestimates the eruption duration. It is likely that the eruption rate for phase 2 of the eruption probably peaked at about 25 m^3 s^{-1} soon after onset and decayed rapidly during the course of the eruption to a more nearly steady state effusion, during which the bulk of the volume was erupted. Short pulses of high eruption rate are suggested by the morphology of Chao I/II. Later effusion rates were probably much lower but probably still higher than the growth rate predicted by the *Kilburn and Lopes* [1991] approach. On this basis we suggest that an eruption duration of about 100 to 150 years for the main phase of Chao is more appropriate. We note that at Santiaguito in Guatemala eruption of lava has continued for 71 years, albeit at a lower rate than we envisage for Chao.

In conclusion, the estimated peak eruption rate (~25 m^3 s^{-1}) for Chao is low in comparison to eruption rates of historic basaltic lava flows like the eruption of Laki, Iceland in 1783 [*Thordarsson and Self*, 1993] but is probably realistic in comparison with observed eruptions of silicic lavas. Low eruption rates are also consistent with the fact that no caldera collapse occurred; rapid eruption of 24 km^3 of magma is likely to have resulted in caldera collapse. We also conclude that the rheological properties of Chao were similar to other silicic lavas. Chao is exceptional, then, only for its volume; few other domes or coulées have volumes close to the minimum 26 km^3 estimate for Chao. All else being equal, slope may have been the crucial factor in determining this.

Assuming a large reservoir of magma is available, the volume of a lava dome erupted onto a flat surface will be limited by the relation between the overpressure driving the eruption and the mass of the lava above the vent. Figure 9 shows that the critical control for effusion of lava is

$$P_e > P_a + \rho g h .$$

Where P_e is the overpressure in the magma chamber, P_a is atmospheric pressure, ρ is the density, g is accelaration due to gravity, and h is the height of the dome. P_e can be assumed to have been similar for each of the lavas, as all came from a coherent magma zone (see below) and there is little difference in vent elevation; Chao has the highest vent elevation of 4950 m, Chillahuita is at ~4750 m, and Tocorpuri and Chason are ~4900 m. Once a critical value of h is reached, no further magma can be erupted. In the case of Chao a large volume of magma was available (see below) and was erupted onto a slope sufficiently steep to allow lava to flow away from the vent area, preventing the critical height from being reached. Observations on the other lava domes in this region suggest the critical height is of the order of 200 m.

Eruption Mechanism

Although there was some explosive activity during the first phase of the Chao eruption, this was volumetrically inconsequential. An outstanding question therefore,is why Chao should have erupted effusively when all the ignimbrites in the region, which it resembles in terms of composition, were erupted explosively. A magma with a moderate water content similar to Chao (~2.5%) should begin to vesiculate rapidly and fragment explosively on ascent as confining pressures decline below 0.1 GPa (1 kbar or ~4 km).

We dismiss the possibility that tephra ejection followed by lava extrusion reflects eruption from a magma zoned in volatiles [*Eichelberger and Westrich*, 1981; *Fink*, 1983], because there is little evidence of zonation in the Chao eruptive products. Another possibility is that an initially volatile-rich silicic magma somehow released its gas as it ascended. A theoretical mechanism for loss of volatiles from a silicic magma during eruption, termed the "permeable foam" model [*Eichelberger et al.*, 1986], has gained widespread support despite objections by *Friedman* [1989] and, more recently, *Fink et al.* [1992]. In this model, an ascending water-rich silicic magma vesiculates to porosities as high as 55-75 vol %, at which point it becomes highly permeable to gas flow due to interconnecting bubbles. *Jaupart and Allegre* [1991] further developed the permeable foam idea, and suggested that

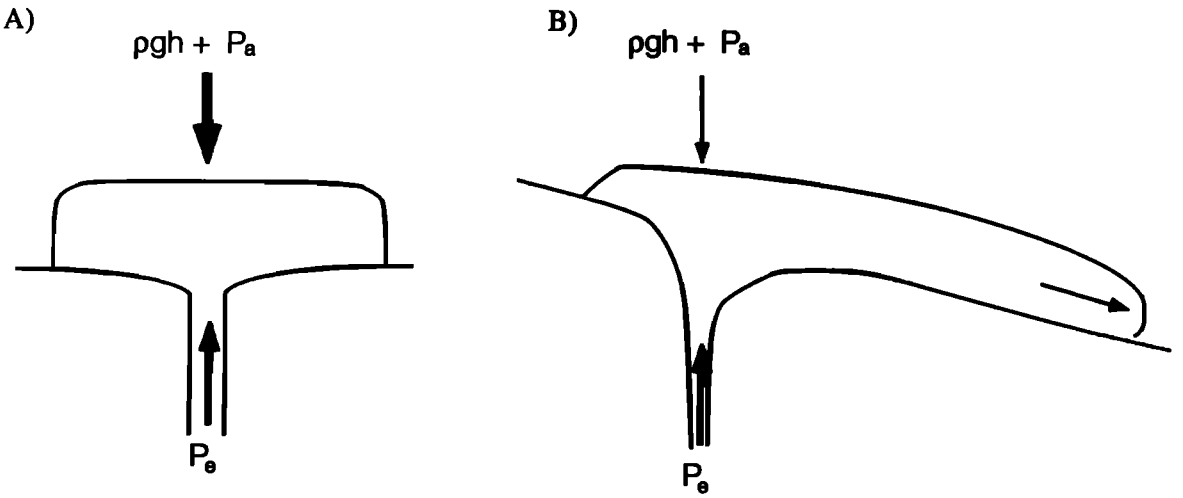

Figure 9. Schematic illustrating pressures involved in eruption of lava onto (a) flat and (b) inclined topography. Eruption is driven by an overpressure P_e and opposed by the pressure of the growing mass of lava above the vent ($\rho gh + P_a$; where ρ is density, g is acceleration due to gravity, h is height of dome and P_a is atmospheric pressure). Length of arrows denotes relative magnitudes of pressure. Note in Figure 9a that once a critical height h is reached, P_e is exceeded and no further lava can be erupted. In Figure 9b, h never reaches a critical value because the lava is continually moving away from the vent area, and P_e is never exceeded.

explosivity of a magma may depend on eruption rate; a slow eruption rate allowing gas to escape from a highly inflated magma through permeable conduit walls. *Jaupart and Allegre* [1991] strengthened their case by demonstrating that the time scales involved in their model are consistent with the slow eruption rates observed for silicic lavas like that of the Mount St. Helens dome.

An implication of the permeable foam model is that silicic lavas should be erupted entirely as highly inflated pumice (55-75 vol % vesicles), which then collapses due to its own weight to form a lava with porosities of less than 5%. At Chao, the initial explosive activity may have served to create a relatively permeable conduit environment in wall rock (probably ignimbrite) where degassing of the magma could take place. A low ascent rate is certainly consistent with our calculations above. However, there are two major objections to the permeable foam model for Chao.

First, it may be difficult to attain the required levels of inflation in crystal-rich magmas. Even if crystallization of the matrix took place after or during emplacement, the phenocryst content of the Chao magma was still very high (50 vol % in some samples). This objection is supported by the poor vesicularity (<30 vol % vesicles) of the pumice associated with Chao. Second, complete preeruption degassing did not occur at Chao, because syneruptive explosive activity proceeded throughout phase 2; thus the magma was not completely degassed, as required by the permeable foam model. We therefore believe it is unlikely that this model is applicable to Chao or, possibly, to other crystal-rich magmas. Further, as we explain below, the apparent high water content of the Chao magma may be a "red herring" and not a factor in its eruption.

We propose that the andesitic inclusions played an important part of the Chao eruption. They are a prominent feature of the later products, appearing in the middle of the sequence (Chao II) and becoming progressively more common in the last stage (Chao III). Their petrologic character, ovoid shapes, vesicular interiors, and chilled margins (Figure 6d) are typical of inclusions resulting from magma mixing throughout the CVZ and elsewhere [e.g., *de Silva et al.*, 1993; *Davidson et al.*, 1990; *Bacon*, 1986]. We interpret these inclusions as evidence that the dacite magma body of Chao was intruded by a hotter, more mafic magma. The appearance of these inclusions toward the middle of the eruption (in Chao II) suggests that the andesite was forcibly injected into, and dispersed throughout, a large part of the chamber as disaggregated blobs. These chilled rapidly in the host dacite, producing the randomly oriented network of acicular crystals in the groundmass (Figure 7d). Xenocrysts in the dacite derived from the mafic magma suggest that complete disaggregation of some blobs occurred. Some phenocrysts from the dacite were also incorporated into the andesite blobs. The record of more mafic rim compositions on the hornblendes and reaction rims of clinopyroxene on quartz is consistent with an increase in temperature either locally or throughout the magma chamber and supports an intrusive event. An alternative argument is that the andesitic inclusions represent a hotter, more mafic layer to the Chao magma chamber, but there is little evidence for a thermally and chemically stratified magma body.

We suggest that the intrusion event may have triggered the eruption of Chao: magma mixing/mingling is a common eruption trigger for volcanic eruptions [cf. *Eichelberger*, 1978; *Sparks et al.*, 1977]. Since the inclusions and host contain similar glass compositions, thermal equilibrium between host and inclusions was reached during the considerable time it took for the Chao eruption to occur.

If the intrusion of the andesite was the eruption trigger, two scenarios can be envisaged.

1. Vesiculation of the inclusions may have resulted in a release of volatiles sufficient to trigger the eruption of Chao and accounting for the first explosive stage of the eruption.

2. Intrusion caused an overpressure in the chamber due to its excess volume [cf. Blake, 1981], and the Chao magma would have been forced out.

A combination of the two scenarios, in which volatile release fueled the initial explosive phase while the later effusions where simply forced out slowly, may be near the truth. In addition, heat added to the system from the andesite itself and from the latent

heat of crystallization may have lowered the bulk viscosity of the Chao magma sufficiently to erupt it. We consider that the intrusion of mafic magma was critical to the eruption of Chao, which otherwise may have stayed below and crystallized as an intrusion; it appears to have been well on the way to complete crystallization.

Other Silicic Lava Bodies in the APVC

Several other beautifully exposed crystal-rich dacite or rhyolite lavas closely similar similar to Chao in age and petrological characteristics occur within 100 km (Figure 10).

Cerro Chillahuita (22°10'S, 68°02'W; Figures 3a and 10a), 20 km east of Chao, and Cerro Tocopuri or La Torta (22°26'S, 67°58'W; Figure 10b), 50 km to the southeast (Figure 2), are circular bodies with areas of ~11 km^2 and volumes of about 4 km^3 each. They have steep, scree-covered flanks about ~200 m high and flat tops and are locally referred to as tortas (cakes). Flow folds rib their upper surfaces. The vent for Chillahuita is clearly visible on the southern side of the lava, which flowed north and eastward spreading down the 3-4° slope (Figure 3a). Tocopuri on the other hand was erupted onto a flat terrain between Volcan Michina (Tocopuri) to the east and Volcan Tatio to the west and is symmetrically arranged about a centrally located vent (Figure 10b). *Marinoviç and Lahsen* [1984] report a K-Ar age of <1 Ma for Tocopuri, which overlies late Pleistocene moraines on its southeastern flank and is thus probably Holocene (<10,000 years) in age.

Both Chillahuita and Tocopuri appear to be the product of single extrusive events. No evidence for explosive activity is observed; a scattered pumice fallout deposit around Chillahuita has the same chemical composition as that on Chao and is probably also from Volcan San Pedro to the west.

Cerro Chascon (21°53'S, 67°54'W; Figure 10c) is located within the Pastos Grandes caldera in Bolivia some 60 km to the north of Chao (2 in Figure 2). It is the largest body in a chain of small silicic bodies known as Cerro Runtu Jarita (Figure 10d) which is probably the surface manifestation of a NW-SE trending dyke similar to that described from the Inyo domes, California [*Fink*, 1985]. Although located within the Pastos Grandes Caldera, these domes are not thought to form part of this caldera complex sensu strictu, however they may be related in a broader sense.

Chascon is a torta with a vent located roughly in its geometric center, from which lava lobes extend radially like petals of a flower. Beneath the lithified basal dome breccia of the lava body is a thin (1 m) rhyolitic pumice fall containing obsidian clasts. Clearly, some minor pyroclastic activity preceded the lava extrusion. Cerro Runtu Jarita consists of seven domes. The two northern domes are extremely crystal-rich dacites, while the southern domes are andesitic. Mixing of the two magma types is ubiquitous throughout (R. Watts and S. L. de Silva unpublished data, 1993).

The other young silicic lava bodies in the region are Cerro Chanka (Pabellon) and two small domes nearby (1 in Figure 2). Chanka is a steep-sided dome consisting of three lobes each with a diameter of ~1.5 km located at 21°48'S, 68°15'W on the western flank of Volcan Azufre. Chanka is not as youthful morphologically as the other domes described. *Roobol et al.* [1974] reported an age of 1.5 ± 0.1 Ma from this center. The two neighboring domes are located on the eastern side of Azufre and are morphologically more youthful than Chanka. The smaller is Cerro Apacheta, a simple dome with a circular plan about 1 km in diameter, while the larger is a composite flow with a quasi-circular plan with maximum diameter of 3 km. Each has the flow-ridged surface typical of silicic lavas.

Like Chao, the vents of all these young silicic centers appear to be controlled by a series of NW-SE trending faults which characterize the tectonic fabric of this part of the APVC (Figure 1). Chillahuita is located just to the north of the line of centers of which Chao forms a part, but it appears to be controlled by the same group of faults. Tocopuri lies at the SE extension of this alignment of volcanoes. Cerro Chascon and the associated Cerro Runtu Jarita domes appear to be the surface manifestation of a NW-SE trending dyke, whereas Cerro Chanka is at the northern extent of the NW-SE trending Inacaliri graben (Figure 2). All these features are located within, or close to, the southern margin of the late Miocene to Pliocene Pastos Grandes caldera complex. The two active geothermal areas of El Tatio (Chile) and Sol de Mañana (Bolivia) lie on the same NW-SE trend (Figure 2).

The Piedras Grandes dome complex is another example of a large silicic lava body in this region. However, this complex is much older, about ~7.5 Ma [*Marinoviç and Lahsen*, 1984], and is an extrusion related to eruption of the Toconce ignimbrite formation [*de Silva*, 1989b]. It is not part of the episode of activity discussed above but is included in the following discussion for comparative purposes.

Relationships Between Lavas and Ignimbrites

Examination of Table 7 reveals that with the exception of Chanka, the young autonomous lava bodies are closely similar in composition. Chao and Chillahuita are particularly striking in the similarity of their trace element and rare earth element (REE) compositions, but all the domes are LREE enriched, with closely similar abundances and therefore similar Ce/Yb and La/Sm; $^{87}Sr/^{86}Sr$ varies from 0.70801 to 0.70805 and $^{143}Nd/^{144}Nd$ from 0.512244 to 0.512247. These chemical characteristics closely resemble those of the older ignimbrites and associated silicic lavas (Table 7), but differ from the silicic lavas erupted from composite cones throughout the CVZ, which have higher large ion lithophile and high field strength element concentrations and lower Sr and higher Nd isotope ratios. Chanka shares the characteristics of the lavas from the composite cones, and this, coupled with its apparent older age, indicates that it does not form part of the recent episode of silicic volcanism we are describing.

Their trace element and isotopic chemistry suggest that the CVZ ignimbrites were produced dominantly by large-scale crustal melting, possibly triggered by mafic magmas from an asthenospheric source. Similar mafic magmas may also rise into the upper crust, experiencing contamination on the way, to feed the magma chambers of the central volcanoes, where further assimilation and fractional crystallization yield small volumes of silicic magma [*de Silva*, 1989a, Figure 5].

The close resemblance in composition of Chao and other young domes to the older ignimbrites demonstrates that silicic magmas of largely similar composition have been erupting in the APVC since the late Tertiary. This combined with the domes' similarity in age, proximity to each other, and their location within the zone of silicic magmatism, allow us to speculate that the domes may represent a discrete new period of silicic magmatism. de Silva [1989a] has argued that the continuing geothermal activity and the presence of the young silicic volcanic products indicate that the silicic magma system beneath the APVC may still be active. Chao and the other domes may be leaks from this large silicic magma system and thus should be regarded as the most recent expression of continuing activity.

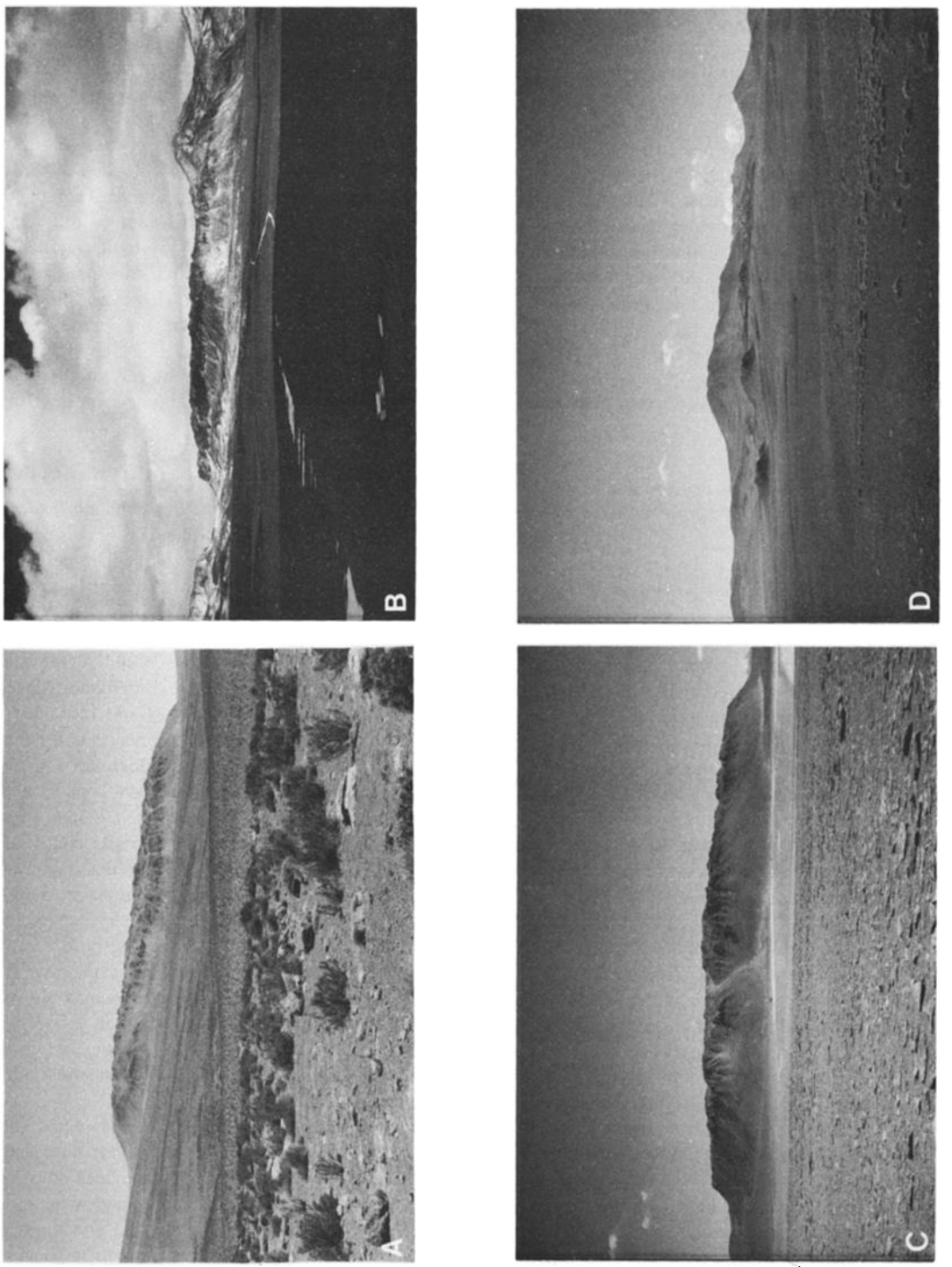

Figure 10. Views of the other young silicic centers in the region. (a) Looking north at Cerro Chillahuita. (b) Cerro Tocopuri from the southwest. (c) View west at Cerro Chascon with Laguna Khara in right middle ground. (d) Looking east at Cerro Runtu Jarita. Cerro Chico in the background.

Table 7. Geochemical Characteristics of Other Young Domes and Silicic Volcanics in the APVC

	Other Domes						Ignimbrites and Associated Domes				Silicic Lavas on Central Volcanoes		
	Chao	Chanka		Chillahuita	Tocopuri	Chascon	Ignimbrites*	Purico D	Piedras Grandes		San Pedro	Chela	Ollague
	88054	CHA-003#	88072	84058	84064	CH89014		7939	84055	84056	7926†	‡CHE-006	‡OLA-031
SiO_2	67.97	65.24	65.09	68.79	71.46	68.17	64.16 - 69.18	63.24	66.05	65.78	66.06	71.8	64.96
TiO_2	0.49	0.52	0.54	0.49	0.37	0.47	0.36 - 0.72	0.72	0.73	0.74	0.49	0.19	0.66
Al_2O_3	15.53	16.07	15.01	15.46	14.96	14.93	14.92 - 16.78	15.45	16.41	16.17	16.89	13.71	16.2
FeO	3.54	3.82	3.95	3.07	2.05	3.07	2.61 - 4.87	5.29	4.84	4.8	3.14	1.03	4.33
MnO	0.06	0.06	0.07	0.06	0.05	0.05	0.06 - 0.09	0.09	0.08	0.08	0.04	0.06	0.06
MgO	1.56	1.60	1.85	1.54	0.99	1.16	1.16 - 2.25	2.4	1.36	1.66	1.33	0.25	1.77
CaO	3.73	3.57	3.55	3.42	2.64	2.82	3.47 - 4.94	4.45	3.7	3.9	3.69	0.7	3.68
Na_2O	3.25	3.98	3.34	3.42	3.34	3.19	3.28 - 3.63	3.04	2.98	2.98	5.27	4.31	4
K_2O	3.81	3.56	3.69	3.66	4.08	4.42	3.21 - 4.06	3.18	3.7	3.72	2.47	4.64	3.57
P_2O_5	0.11	0.15	0.07	0.1	0.06	0.11	0.09 - 0.19	0.18	0.16	0.17	0.17	0.05	0.19
Rb	158	138	181	168	181	257	148 - 241	149	166	166	48	124	116
Sr	335	493	359	325	284	267	240 - 448	304	308	313	792	90	460
Ba	610	903	712	600	668	588	453 - 740	453	615	611	1021	1048	958
Y	17	15	15	16	14	15	16 - 25	26	23	22	9	10	17
Zr	150	162	151	128	104	158	124 - 181	146	147	127	139	124	200
Nb	14	9	13	12	11	17	11 - 18	14	14	14	5	12	13
Th	28		31	27	26	30	11 - 23	18	19	19	4		
Ni	25	7	13	24	19	21	34 - 9	30	29	29	27	3	7
Cr	37	11	35	43	38	14	13 - 60	74	63	61	48	6	25
Ce/Yb	48.37			48.54	58.93		35.4 - 59.2			39.23			
La/Sm	8.1			8.12	10.7		7.45 - 12.4			6.11			
Ta	1.43			1.43	1.45		0.72 - 1.77			1.54			
Hf	4.46			4.48	3.45		4.34 - 5.87			5.48			
Cs	14			14.3	12		4.02 - 11.1			18			
Sc	7			7.1	4.5		3.9 - 12.0			11.5			
$^{87}Sr/^{86}Sr$	0.70806	0.70606		0.70805	0.70801		0.70829 - 0.70970			0.70903	0.70660	0.70580	0.70778
$^{143}Nd/^{144}Nd$	0.51224			0.51224	0.51225		0.51209 - 0.51227						

Sample CHE-006 is a pumice; sample OLA-031 is dacite dome. Major elements are in weight percent; others are in parts per million.

*Data from de Silva [1987]

† Lava dome on Volcan San Pedro [O'Callaghan and Francis, 1986]

‡Data from Wörner et al. [1992]

Regional Significance of the Young Silicic Lavas

Given that the other young silicic lavas all share a general family resemblance and may represent the same magmatic episode, is it possible that intruding mafic magma was as important in their eruptions as at Chao? Recent work at Chascon and Runtu Jarita where magma mixing is abundant, certainly implicates this as an eruption trigger (R. Watts and S. L de Silva, unpublished data, 1993). All the lavas appear to be in an advanced stage of evolution, and there seems little likelihood they would have erupted without some trigger. We note that periodic intrusions of mafic magma are thought to be an important feature in the long term evolution of large continental silicic magmatic provinces [cf. Hildreth, 1981]. We conclude that intrusion of mafic magma was likely to have been the eruption trigger.

If the young silicic lavas described here do indeed represent a discrete new episode of leakage from a regional silicic magma reservoir, two interesting possibilities emerge. On the one hand, the episode may constitute the waning stages of the magmatic system. In this case, the dacite lavas represent "residual" volatile-poor magma left behind after the massive explosive eruptions that produced the ignimbrites and then refueled by intruding mafic magma. In this case, the moderate water content of the dacites inferred from their mineralogy would be an artefact of the original magma, and therefore a "red herring" that is not relevant to the eruption mechanism of the lavas.

On the other hand, the young dacitic lavas may herald birth of a "new" growing silicic magma system beneath the APVC, produced in response to the melting of upper crustal material (probably the plutonic equivalents to the ignimbrites) by mantle-derived mafic magmas. Either of these scenarios would explain why essentially similar magmas erupted explosively over a period of 10 m.y. as huge volumes of ignimbrite during the early history of the magma system, followed by small, quiet effusions in this last episode we are describing.

It is not clear which of these is more likely. The interval between the last major ignimbrite eruption and the eruption of Chao is about 1 m.y., and volatile-depleted magma would probably have solidified during this time. In this light, the remelting scenario becomes more appealing but is problematic because it is difficult to see how phenocrysts such as hornblende are preserved without resorption. Further work is needed to resolve these issues, but in either case, Chao and its neighbors may define the extent of the presently active magmatic system and, in the latter case, may indicate the location of a future caldera.

Summary and Conclusions

Chao is an exceptionally large volume, composite coulée composed of homogeneous, crystal-rich, dacite. Its eruption proceeded in three main phases; a short initial explosive phase was followed by two dominantly effusive phases during which over 90% of the magma was erupted. Chao is similar to other silicic lava bodies in rheologic and eruptive parameters. Inclusions in the later erupted portions of the lava suggest that its eruption was triggered by intrusion of mafic magma into a homogeneous crystal-rich dacite magma body. Chao is thought to have been emplaced over a period of about 100 to 150 years, with maximum effusion rates of about 25 m^3 s^{-1}. The local topographic slope led to the formation of large coulées rather than small domes. Petrologic and physical similarities between Chao and neighboring young domes suggest they form part of the same magmatic episode. Their general family resemblance with the older regional ignimbrites suggests that all form part of a long lived silicic magmatic system below the APVC. Chao and the other young domes may have been derived from a waning magmatic system containing "old" volatile-poor silicic magma left after eruption of the voluminous ignimbrites. Alternatively, they may represent a new crustal melting episode fueled by intrusion of fresh hot mafic magma. The location of the young silicic lavas probably defines the extent of the presently active magmatic system and may indicate the location of a future caldera.

Acknowledgements. An early version of this manuscript benefited from thorough and insightful reviews by Jon Fink, Don Swanson, and Mike Sheridan. These, discussions with Bill Rose, Jon Fink, Curtis Manley, and Stephen Blake as well as official reviews by Curtis Manley and John Eichelberger have improved this work immeasurably. Fieldwork was conducted in several stages but largely under the auspices of NASA grant NAGW-1167 while S. de S. and P.W.F. were at the Lunar and Planetary Institute (LPI) in Houston. The LPI is operated by the University Space Research Association under NASA contract NASW-4066. Lindsey O' Callaghan, Jon Davidson (UCLA), and Peter Mouginis-Mark (University of Hawaii) are thanked for field support during various campaigns between 1985 and 1989. This paper is SOEST contribution #3549.

References

Anderson, D.J., and D.H. Lindsley, New (and final!) models for Ti-magnetite/ilmenite geothermometer and oxygen barometer (abstract), *Eos Trans. AGU, 66*, 416, 1985.

Bacon, C.R., Magmatic inclusions in silicic and intermediate volcanic rocks, *J. Geophys. Res., 91*, 6091-6112, 1986.

Blake, S., Volcanism and the dynamics of open magma chambers, *Nature, 289*, 783-785, 1981.

Blake, S., Viscoplastic models of lava domes, in *Lava Flows and Domes: Emplacement Mechanism and Hazard Implications* , IAVCEI Proc. in Volcanol. vol. 2, edited by J . Fink,. pp.88-126, Springer-Verlag, New York, 1990.

Bonnichsen, B., and D.F., Kauffman, Physical features of rhyolite lava flows of the Snake River Plain volcanic province, southwestern Idaho, in*The Emplacement of Domes and Silicic Lava Flows*, edited by J. Fink, *Spec. Pap. Geol. Soc. Am. 212*, 119-145, 1987.

Davidson, J.P., S.L. de Silva, P. Holden, and A.N. Halliday, Small-scale disequilibrium in a magmatic inclusion and its more silicic host. *J. Geophys. Res., 95*, 17,661-17,675. 1990.

de Silva, S.L., Large-Volume Explosive Silicic Volcanism in the Central Andes, Unpub. Ph.D. thesis, 304 pp. Open University, Milton Keynes, England, 1987

de Silva, S.L., Altiplano-Puna volcanic complex of the Central Andes, *Geology, 17*, 1102-1106, 1989a.

de Silva, S.L., Geochronology and stratigraphy of the ignimbrites from the 21°30'S to the 23°30'S portion of the Central Andes of N. Chile, *J. Volcanol. Geotherm. Res., 37*, 93-131, 1989b.

de Silva, S.L., and P.W. Francis, *Volcanoes of the Central Andes*, 213 pp. Springer-Verlag, New York, 1991.

de Silva , S.L., S. Self, and P.W. Francis, The Chao dacite revisited (abstract) *Eos Trans. AGU, 69*, 1487-1488, 1988.

de Silva, S.L., J.P. Davidson, I.C. Croudace, and A. Escobar, Volcanologic and petrologic evolution of volcan Tata Sabaya, S.W. Bolivia, *J. Volcanol. Geotherm. Res., 53*, 305-335, 1993.

Dragoni, M., and A. Tallarico, Effect of crystallization on the rheology and dynamics of lava flows, *J. Volcanol. Geotherm. Res., 59*, 441-452, 1994.

Eichelberger, J.C., Vesiculation of mafic magma during the replenishment of silicic magma reservoirs, *Nature, 288*, 446-450, 1978.

Eichelberger, J.C., and H.R. Westrich, Magmatic volatiles in explosive rhyolitic eruptions. *Geophys. Res. Lett., 8*, 757-760, 1981.

Eichelberger, J.C., C.R. Carrigan, H.R. Westrich, and R.H. Price, Non-explosive silicic volcanism, *Nature, 323*, 598-60, 1986.

Fink, J.H., Surface folding and viscosity of rhyolite flows, *Geology, 8*, 250-254, 1980.

Fink, J.H., Structure and emplacement of a rhyolitic obsidian flow: Little Glass Mountain, Medicine Lake Highland, Northern California, *Geol. Soc. Am. Bull., 94*, 362-380, 1983.

Fink, J.H., Geometry of silicic dikes beneath the Inyo domes, California, *J. Geophys. Res., 90*, 11127-11133, 1985.

Fink, J.H., and R.W. Griffiths, A laboratory analog study of the morphology of lava flows extruded from line and point sources. *J. Volcanol. Geotherm. Res., 54*, 19-32, 1992.

Fink, J.H., S.W. Anderson, and C.R. Manley, Textural constraints on silicic volcanism: beyond the permeable foam model. *J. Geophys. Res., 97*, 9073-9083, 1992.

Friedman, I., Are extrusive rhyolites produced from permeable foam eruptions? *Bull. Volcanol., 51*, 69-71, 1989.

Griffiths, R., and J. Fink, Effects of surface cooling on the spreading of lava flows and domes. *J. Fluid Mech.., 252*, 667-702, 1993.

Guest J.E., and J. Sanchez, A large dacitic lava flow in Northern Chile, *Bull. Volcanol., 33*, 778-790, 1969.

Heiken, G., and J.C. Eichelberger, Eruptions at Chao Crags, Lassen Volcanic National Park, California, *J. Volcanol. Geotherm. Res., 7*, 443-481, 1980.

Henry, C.D., and J.A. Wolff, Distinguishing strongly rheomorphic tuffs from extensive silicic lavas, *Bull. Volcanol., 54*, 171-186, 1992.

Henry, C.D., J.G. Price, J.N. Rubin, D.F. Parker, J.A. Wolff, S. Self, R.R. Franklin, and D.S. Barker, Widespread lava-like volcanic rocks of the Trans-Pecos Texas, *Geology, 16*, 509-512, 1988.

Hildreth, E.W. Gradients in silicic magma chambers: Implications for lithospheric magmatism, *J. Geophys. Res., 86*, 10,153-10,192, 1981.

Hollingworth, S.E., and J.E. Guest, Pleistocene glaciation in the Atacama desert, Northern Chile, *J. Glaciol., 6*, 749-751, 1967.

Hulme, G., and G. Fielder, Effusion rates and rheology of lunar lavas. *Philos. Trans. R. Soc. London., A , 285*, p. 227-234, 1977.

Huppert, H.E., J.B. Shepherd, H. Sigurdsson, and R.S.J. Sparks, On lava dome growth with application to the 1979 lava extrusion of the Soufriere of St. Vincent, *J. Volcanol. Geotherm. Res., 14*, 199-222, 1982.

Jaupart, C., and C. Allegre, Gas content, eruption rate, and instabilities of eruption regime in silicic volcanoes, *Earth Planet. Sci. Lett., 102*, 413-429, 1991.

Johnson, M., and M. Rutherford, Experimentally determined conditions in the Fish Canyon Tuff, Colorado, magma chamber, *J. Petrol., 30*, 711 - 737, 1989.

Kilburn, C.J., and R.M.C. Lopes, General patterns of flow field growth: aa and blocky lavas, *J. Geophys. Res., 96*, 19,712-19,732, 1991.

Manley, C.R., Extended cooling and viscous flow of large, hot rhyolite lavas: Implications of numerical modelling results. *J. Volcanol. Geotherm. Res., 53*, 27-46, 1992.

Marinoviç, N., and A. Lahsen, Hoja Calama. Region de Antofagasta, scale 1:250,000 carta geologica de Chile 58, *Serv. Nac. Geol. Min.*, Santiago, 1984.

Marsh, B.D., On the crystallinity, probability of occurrence and rheology of lava and magma, *Contrib. Mineral. Petrol., 78*, 85-98, 1981.

McBirney, A.R., and T. Murase, Rheological properties of magmas, *Annu. Rev. Earth Planet. Sci., 12*, 337-357, 1984.

Moore, H.J., D.W.G. Arthur, and G.G. Schaber, Yield strengths of flows on the Earth, Mars, and Moon, *Proc. Lunar Planet. Sci. Conf., 9th*, 3351-3378, 1978.

Naney, M.T., Phase equilibria of rock-forming ferromagnesian silicates in granitic systems, *Am. J. Sci., 283*, 993-1033, 1983.

O'Callaghan, L. J., and P.W. Francis, Volcanological and petrological evolution of San Pedro volcano, Provincia El Loa, north Chile, *J. Geol. Soc. London., 143*, 275-286, 1986.

Pinkerton, H., and R.J. Stevenson, Methods of determining the rheological properties of magmas at sub-liquidus temperatures, *J. Volcanol. Geotherm. Res., 53*, 47-66, 1992.

Roobol, M.J., P.W. Francis, W.I. Ridley, M. Rhodes, and G.P.L. Walker, Physico-chemical characters of the Andean volcanic chain, between latitudes 21° and 22° south, paper presented at Symposium Internacional de Volcanologia, Int. Assoc. of Volcanol. and Chem, of Earth's Inter., Santiago, Chile, Sept. 9-14th, 1974.

Rose, W.I., Volcanic activity at Santiaguito, 1976-1984, in *The Emplacement of Domes and Silicic Lava Flows*, edited by J. Fink, *Spec. Pap. Geol. Soc. Am., 212*, 17-28, 1987.

Sparks, R.S.J., H. Sigurdsson, and L. Wilson., Magma mixing as a mechanism for triggering acid explosive volcanic eruptions, *Nature, 267*, 315-318, 1977.

Spencer, K.J., and D.H. Lindsley, A solution model for coexisting iron-titanium oxides, *Am. Mineral., 66*, 1189-1201, 1981.

Stasiuk, M.V., C. Jaupart, and R.S.J. Sparks, On the variation of flow rate in non-explosive lava eruptions, *Earth Planet. Sci. Lett. 114*, 505-516, 1993.

Stormer, J.C., The effects of recalculation on estimates of temperature and fugacity from analyses of multicomponent iron-titanium oxides, *Am. Mineral., 68*, 586-595, 1983.

Swanson, D.A., D. Dzurisin, R.T. Holcomb, E.Y. Iwatsubo, J.J. Chadwick, Jr., T.J. Casadevall, J.W. Ewert, and C.C. Heliker, Growth of the lava dome at Mount St Helens, Washington, (USA), 1981-1983. in *The Emplacement of Domes and Silicic Lava Flows*, edited by J. Fink, *Spec. Pap. Geol. Soc. Am. 212*, 119-145, 1987.

Thordarsson, T., and S. Self, The Laki (Skaftár Fires) and Grimsvotn eruptions in 1783-85, *Bull. Volcanol., 55*, 233-264, 1993.

Wadge, G., The variation of magma dsicharge during basalticc eruptions, *J. Volcanol. Geotherm. Res., 11*, 139-168, 1981.

Walker, G.P.L., Lengths of lava flows, *Philos. Trans. R. Soc. London, A, 274*, 484-495, 1973.

Wilson, L., and J.W. Head, A comparison of volcanic eruption processes on Earth, Moon, Mars, Io and Venus. *Nature, 302*, 663-669, 1983.

Wörner, G., S. Moorbath, J. Entemann, L. Lopez-Escobar, S. Horn, R.S. Harmon, and J.P. Davidson, Variaciones Geoquimicas, locales y regionales, en el frente volcanico cuaternario de los Andes Centrales (17° 30'-22°00'S), norte de Chile, *Rev. Geol. Chile, 19*, 37-59, 1992.

S.L. de Silva, Department of Geography and Geology, Indiana State University, Terre Haute, IN 47089. (e-mail: gesilva@scifac.indstate.edu)

R.E. Drake, Berkeley Geochronology Center, Berkeley, CA 94720

P.W. Francis, Department of Earth Sciences, Open University, Milton Keynes, MK7 6AA, England. (e-mail: P.W.Francis@open.ac.uk)

C. Ramirez R, Servicio Nacional de Geologia y Mineria, Casilla 2032, Santiago, Chile.

S. Self, Hawaii Center for Volcanology, Department of Geology and Geophysics, SOEST, University of Hawaii, Honolulu, HI 96822. (e-mail: self@soest.hawaii.edu)

(Received June 14, 1993; revised February 25, 1994; accepted March 7, 1994.)